

JGR Atmospheres

RESEARCH ARTICLE

10.1029/2021JD035227

Key Points:

- With increasing PM_{2.5}, summer urban heat island intensity (UHII) weakens and winter UHII strengthens
- Winter PM_{2.5} pollution weakens the UHII at night but strengthens it during daytime
- PM_{2.5} affects UHII via aerosol-radiation interaction in summer and via aerosol-planetary boundary layer interaction in winter

Supporting Information:

Supporting Information may be found in the online version of this article.

Correspondence to:

G. Ren,
guoyoo@cma.gov.cn

Citation:

Yang, G., Ren, G., Zhang, P., Xue, X., Tysa, S. K., Jia, W., et al. (2021). PM_{2.5} influence on urban heat island (UHI) effect in Beijing and the possible mechanisms. *Journal of Geophysical Research: Atmospheres*, 126, e2021JD035227. <https://doi.org/10.1029/2021JD035227>

Received 12 MAY 2021

Accepted 25 AUG 2021

PM_{2.5} Influence on Urban Heat Island (UHI) Effect in Beijing and the Possible Mechanisms

Guowei Yang¹ , Guoyu Ren^{1,2} , Panfeng Zhang^{1,3} , Xiaoying Xue¹ , Suonam Kealdrup Tysa¹, Wenqian Jia¹, Yun Qin¹ , Xiang Zheng¹, and Siqi Zhang^{1,2}

¹Department of Atmospheric Science, School of Environmental Studies, China University of Geosciences, Wuhan, China, ²Laboratory for Climate Studies, National Climate Center, China Meteorological Administration, Beijing, China,

³School of Tourism and Geographical Sciences, Jilin Normal University, Siping, China

Abstract Whether the urban heat island (UHI) is affected by air pollution in urban areas has attracted much attention. By analyzing the observation data of automatic weather stations and environmental monitoring stations in Beijing from 2016 to 2018, we found a seasonally dependent interlink of the UHI intensity (UHII) and PM_{2.5} concentration in urban areas. PM_{2.5} pollution weakens the UHII in summer and winter night, but strengthens it during winter daytime. The correlation between the UHI and PM_{2.5} concentration has been regulated by the interaction of aerosol with radiation, evaporation and planetary boundary layer (PBL) height. The former two change the surface energy balance via sensible and latent heat fluxes, while the latter affects atmospheric stability and energy exchange. In summer daytime, aerosol-radiation interaction plays an important role, and the energy balance in urban areas is more sensitive to PM_{2.5} concentration than in rural areas, thereby weakening UHII. In winter daytime, aerosol-PBL interaction is dominant, because aerosols lower the PBL height and stabilize atmosphere, weaken the heat exchange with the surrounding, with more heat accumulated in the urban areas and the increased UHII. Changes in evaporation and radiation strengthen the relationship. At night, the change of UHII more depends on the energy stored in the urban canopy. Aerosols effectively reduce the incident energy during daytime, and the long-wave radiation from the buildings of urban canopy at night becomes less, leading to a weakened UHII. Our analysis results can improve the understanding of climate-aerosols interaction in megacities like Beijing.

Plain Language Summary A detailed understanding of the relationship between PM_{2.5} and the urban heat island (UHI) effect is significant for climate change adaption, planning, and sustainable development in urban regions. While Beijing is among the cities with the highest population densities and fastest urbanization rates in China and even the world, the impacts of PM_{2.5} pollution on UHI remain unclear, and the works using different methods (observations or models), observational data (stations or satellites) and the selecting procedures to classify stations deliver different results. This study demonstrates that the UHI intensities in summer and winter, respectively, exhibit weakening and strengthening tendency as PM_{2.5} concentration increases. These effects are modulated by aerosol-radiation interaction in summer and winter, and aerosol interaction with planetary boundary layer and evaporation in winter. Our analysis improves the understanding of interaction of urban climate and air pollution.

1. Introduction

Urbanization has caused tremendous changes in the structure, properties, and spatial distribution of urban underlying surface, resulting in huge differences in land surface properties between rural and urban areas (Kalnay & Cai, 2003; Monteith & Oke, 1980; Oke, 1976, 1982; P. Yang et al., 2017; Ren et al., 2008; Shepherd et al., 2010; Zhao et al., 2014; Zhou et al., 2016). The change of the surface from natural to impervious surface modifies the surface characteristics, causing the decrease of surface albedo and the increase of Bowen ratio (the ratio of sensible heat flux to latent heat flux), and also an increase of surface energy storage in urban areas (Chakraborty et al., 2017; Rizwan et al., 2008). The alternation of surface heat budget forms the urban heat island (UHI), which makes urban areas warmer than surrounding rural areas (Oke, 1982; Ren & Zhou, 2014; Yang et al., 2013). Studies show that UHI has obvious diurnal and seasonal variation characteristics (Rosenzweig et al., 2005; Yang et al., 2013).

Many factors, including weather and climate conditions, urban impervious surface, heights of buildings and anthropogenic heat release, affect the diurnal and seasonal pattern of UHI (Ding et al., 2016; Oke, 1982; Ryu & Baik, 2012; Yang et al., 2019; Y. Yang et al., 2020; Yao et al., 2017, 2018; Zhou et al., 2014). The most remarkable UHI can be observed on calm and clear winter nights in large cities (Jia et al., 2019; P. Yang et al., 2013, 2017). The main factors that influenced the daytime UHI are the increase of Bowen ratio and the related reduction of evaporative cooling efficiency in urban land. At night, the heat released from buildings and energy use is the main cause leading to urban warming (Taha, 1997; Voogt & Oke, 2003; Zhao et al., 2014).

Pollutant emission is another important aspect of human activities in urban areas (McDonnell & MacGregor-Fors, 2016). Because of their complex composition and properties, the pollutants or aerosol particles will reduce air quality, change the physical and chemical characteristics of the atmosphere, and endanger human health (Cohen et al., 2017; Durant et al., 1999; Hamilton & Mansfield, 1991; Künzli et al., 2000). Aerosol particles can also alter the radiation balance of the atmosphere and the surface, decreasing the shortwave radiation reaching the ground and thus producing a cooling effect on the ground. However, they are more effective than water vapor and greenhouse gas in absorbing and releasing radiation under certain conditions (Jacobson, 1998; Kuhlbusch, 1998; Rosen et al., 1978) and thus may increase the longwave radiation energy received on the urban surface. The overall effect depends on the initial particle size at the time of emission and the size growth due to aging and water vapor absorption (Ramanathan et al., 2001).

The microphysical effects of aerosols can also influence cloud properties and precipitation conditions (Li et al., 2011; Rosenfeld et al., 2008), reduce the frequency of light rain but increase heavy rainfall in humid areas (P. Yang et al., 2017), and change air convection by weakening the vertical temperature gradient (Ding et al., 2016; Gu et al., 2010; Huang et al., 2018; Li et al., 2017). The increase in total and intense precipitation in urban areas and downwind areas of large cities has been observed, and this may have been related to the stronger convective activities and the increase of aerosols in summer (P. Yang et al., 2017).

UHI and air pollution are not independent, to the point that where UHI exists, air pollution is likely to occur (Crutzen, 2004). The emergence of UHI is often accompanied by higher temperature, and the higher temperature can accelerate the photochemical reaction, leading to secondary pollutants (Wang et al., 2018). Diurnal variation of UHI also has an important impact on the air pollutants, which may change the spatial distribution and availability of regional pollutants (Sarrat et al., 2006). Moreover, UHI and air pollution are both closely related to anthropogenic heat release from transport, industry and other human activities like central heating and residential coal combustion. With development of urban areas or urbanization, the UHI intensity and the aerosol particle concentration may simultaneously increase, and they may interact to produce a complex thermal-dynamic condition of the planetary boundary layer (PBL) over the big cities. In addition, the UHI can increase the heat stress of urban residents (Gabriel & Endlicher, 2011), and the synergy of heat stress and air pollution can make people more vulnerable to their respective threats (Lai & Cheng, 2010). To have more insight into the relationship between aerosol particles and the UHI effect is of great significance for understanding urban climate and climate change, and also for well-being of urban residents and urban planning.

Previous studies have shown that aerosol particles intensify the UHI effect, warm the atmosphere, change the stability of the PBL (Menon, 2002) and reduce the diurnal temperature change (Travis et al., 2002) over the urban areas. In Dar es Salaam, Tanzania, and Shenyang, China, nocturnal UHII showed positive correlation with total suspended particulate (TSP) concentration (Jonsson et al., 2004; Zhang et al., 2004). A study conducted in Thessaloniki in summer proved that worse air quality is directly related to higher UHI intensity (UHII) (Poupkou et al., 2011). Li et al. (2007) pointed out that the pollution zone is also the center of the UHI in Beijing, and suggested that they may have a causal relationship. Chen et al. (2018) found that the UHII of Beijing increased by 16.7% during the winter polluted days. Zheng et al. (2018) pointed out that aerosols strengthen the UHII throughout the day, especially at night in Beijing.

However, some studies also demonstrated the opposite effects of particulate matter. The dust dome formed by suspended particulate matter above a city may lead to an imbalance in the energy balance of the urban boundary layer system via affecting the radiation process, resulting in a positive correlation between TSP and urban cool island (Sang et al., 2000). High-concentration aerosols in the urban boundary layer may

cause an additional cooling effect during the daytime (Chen et al., 2003). Of course, shadows from high-rise buildings in the city center may also be another reason for the daytime urban cool island (X. Yang et al., 2017). Wu et al. (2017, 2021) revealed that fine particles weakened the UHII during the day, but the reduction mainly occurred at altitudes below 500–1,000 m. The nighttime UHII weakens first and then strengthens with the increase of pollution level. Y. Yang et al. (2020) showed that aerosol radiation interaction (aerosol-cloud interaction) regulates and reduces the winter UHI intensity in Beijing, with the UHII at the time of daily maximum/minimum temperature exhibiting a decreasing/increasing tendency as PM_{2.5} concentration increases. Yu et al. (2020) analyzed the mechanisms of the impacts of aerosols and urbanization using model, and found that aerosols reduced urban-related warming during the daytime by 20% as fine particles concentrations increased and also enhanced urban-related warming at dawn conversely. Li et al. (2018, 2020) examined potential interactions between urban pollution islands and UHI in Berlin, Germany, and found that urban pollution islands are negatively correlated with atmospheric UHI, but they cause higher surface UHI at night.

Land surface temperatures are determined by and respond to land surface — atmosphere interactions (Jin & Dickinson, 2010; Jin et al., 1997). Satellite-derived land surface temperature (T_{skin}) data have also been employed to compare with atmosphere temperature (T_{air}) and investigate the surface UHI phenomenon (Cao et al., 2016; Chakraborty & Lee, 2019; Chakraborty, Lee, & Lawrence, 2021; Chakraborty, Sarangi, & Lee, 2021; Jin & Dickinson, 2010; Jin & Shepherd, 2005; Jin et al., 1997, 2010, 2011; Mildrexler et al., 2011; Zhao et al., 2014). Satellite T_{skin} data enables easy assessments of surface UHIs across cities worldwide (Clinton & Gong, 2013; Imhoff et al., 2010; J. Peng et al., 2018; S. Peng et al., 2012). Wang et al. (2017) compared atmospheric UHI and found that both exhibited significant seasonal and diurnal cycles and surface UHI showed stronger seasonal cycles during the daytime. Jin et al. (2010, 2011) examined the interconnection between urban heat and pollution islands in Shanghai by combining the satellite data (MODIS) of surface temperature, aerosols, water vapor, cloud fraction, and land cover. They found that aerosols decreased the urban surface temperature of Beijing and New York by reducing incident radiation. Pandey et al. (2012) mapped day and night time thermal pattern of Delhi with MODIS satellite data and revealed the formation of daytime cool island over central parts of the city, with the high values of particulate matter during low wind conditions favoring the development of the so-called cool island effect. Cao et al. (2016) studied the relationship between aerosol pollution and surface UHI in China's cities with different sizes, showing a contribution of aerosol to night UHI intensity being 0.7 ± 0.3 K. Han et al. (2020) analyzed 35 Chinese cities with rapid urbanization based on the WRF-Chem model and showed that there were differences in the impact of particulate matter on daytime surface UHI in different seasons: surface UHI intensity decreased in summer and increased in winter.

Up to now, however, there are different or even opposite conclusions about the impact of particulate matter on air or surface UHI. Under the same geographical and climatic conditions, the influence of particulates on UHI in different seasons still needs further research.

In this study, we applied the data of the high-density automatic weather stations (AWSs) and environmental monitoring stations in Beijing to examine the possible effect of PM_{2.5} concentration on UHI intensity. While the previous studies UHI involve both atmospheric and surface UHI, this study focuses on atmospheric UHI. Our analysis showed a complex mechanism of the aerosols on the UHI and thermal environment of the city's canopy.

2. Study Area, Observation Data, and Methodology

2.1. Study Area

The total area of Beijing is about 16,000 km². As of 2018, the permanent resident population of Beijing has exceeded 21 million, including about 18 million in urban areas, and the urbanization rate has reached 86.6%. It is located in the north of the Northern China Plain, south of Yan'an Mountains. The plain area accounts for about 38.8% of the total area, and the altitude of most areas is lower than 100 m.

With the growth of the economy and population, Beijing has experienced a rapid urbanization. There is a multi-ring road traffic system (as shown in Figure S1), with the areas within different ring roads representing the different urban areas. In this study, the stations located in the Sixth Ring Road of Beijing are

considered as urban stations, while the stations located in the Fourth Ring Road are considered as the central urban stations.

2.2. Observational Data

China's land use data in 2015 are used in this study, which included six first-class types of cropland, woodland, grassland, water area, residential land, and unused land, and 25 second-class types. The data is provided by Resource and Environment Science and Data Center (<http://www.resdc.cn/>) with a spatial resolution of 1×1 km.

The daily observed temperature (average, maximum and minimum temperature), wind speed, and wind direction data of AWS in Beijing during 2016–2018 were obtained from the National Meteorological Information Center (NMIC) of China Meteorological Administration (CMA), daily time range is from 08:00 of the day to 08:00 of the next day. There are totally 438 AWSs in the study region. The height of the AWS temperature sensor from the ground is 2 m, which is consistent with the height of the manual stations. The NMIC carried out preliminary quality control for the data, and the possible wrong records have been checked and corrected (Ren & Xiong, 2007; Ren et al., 2015).

Besides, the surface solar radiation is only recorded at the Beijing station (BJ, 54511), a national reference climate station located in the urban area of Beijing. To eliminate the influence of morning fog and solar radiation diurnal variation (i.e., low solar radiation in the early morning and late afternoon), the radiation data only from 09:00 to 16:00 LST was selected as daytime radiation, and the radiation data from 21:00 LST on the same day to 04:00 LST the next day was selected as night radiation to explore the relationship between downward short wave radiation and particulate matter concentration at Beijing station. ERA5-Land reanalysis data set has hourly temporal resolution and $0.1^\circ \times 0.1^\circ$ (native resolution is 9 km) horizontal resolution. The radiation data from the reanalysis are used to make up for the lack of observation data through the method of sampling at the location of the observational station. Table S1 shows the comparison of the observational reanalysis values at the location of Beijing station, and they have a high correlation.

Beijing station is considered as the representative station of the Beijing area in the study. The observed daily wind speed, wind direction, and weather process records are used to represent the characteristics of the relevant meteorological elements in the whole research area. The L-band sounding data mentioned below also comes from the radiosonde of Beijing station, which contains high-resolution profiles of temperature, pressure, relative humidity, wind speed, and wind direction at 08:00 Beijing time. Moreover, pan-evaporation data from Beijing Station and Miyun Station (MY, 54416) will also be used in this research.

$\text{PM}_{2.5}$ concentration data were used to represent particulate matter, which is from Beijing Municipal Ecological and Environmental Monitoring Center. The center will publish real-time hourly $\text{PM}_{2.5}$ concentration data of 35 national and provincial air quality monitoring stations in Beijing. See Table S2 for station information. To better characterize the regional air quality, the stations within the Sixth Ring Road are selected as the urban stations to calculate the average $\text{PM}_{2.5}$ concentration in Beijing urban area.

2.3. Methodology

2.3.1. Methods of Data Quality-Control and Classification of Urban and Rural Stations

The data quality control of automatic stations is made referring to the statistical regulation of 24 times of regular record average value in "Specifications for Surface Meteorological Observation", and the stations that pass the quality inspection are selected for use. The regulations of statistical records are as follows:

In a month, when a certain fixed time record is missing for seven times or less, the monthly statistics shall be made according to the actual records at each fixed time, and the monthly statistics shall not be made for the fixed time when there are eight or more missing measurements.

The statistical method of monthly average: in a month, if there are six or fewer missing measurements for each fixed time average, the daily and monthly average shall be calculated according to the actual fixed time average; if there are seven or more missing measurements, the corresponding monthly average shall be

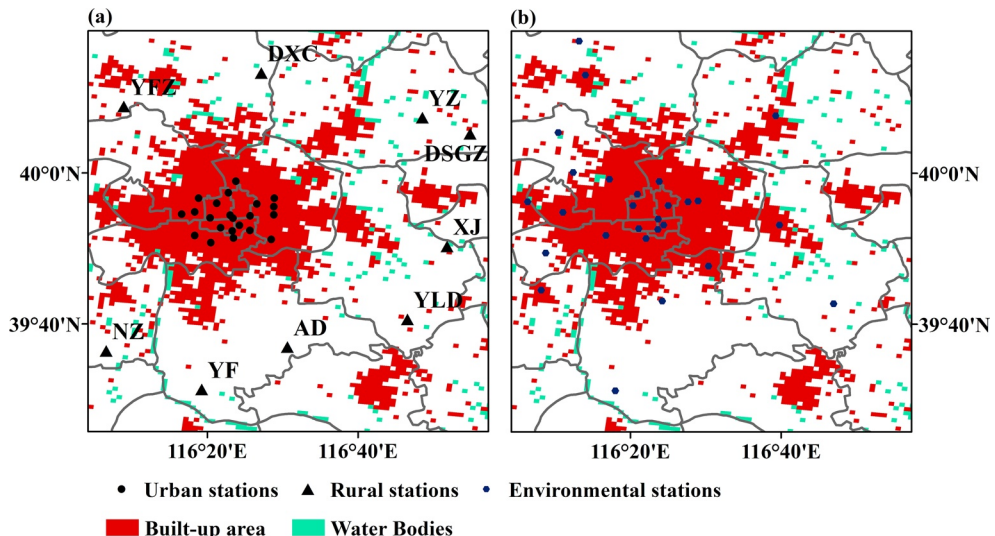


Figure 1. Distribution of different types of stations in Beijing Municipality. (a) Location of urban and rural stations in automatic weather stations. (b) Location of environmental monitoring stations. Red area indicates built-up area and aqua green area indicates water bodies.

regarded as the missing measurement. If the data of a certain month of a site does not conform to the above principles, the site will be abandoned.

According to the above criteria, a total of 139 automatic stations with altitudes less than 120 m are screened out (Figure S1). In this study, to better reflect the intensity of UHI, 22 central urban stations within the Fourth Ring Road are selected as urban stations. The built-up area in the land use data of Beijing in 2015 is extracted, and the buffer zones with radii of 1, 2, 3, 4, and 5 km are respectively made with each automatic station as the center of the circle (Figure S2). The percentage of urban land use in each buffer zone is calculated. The sites with the percentage of urban land use less than 5% within the radius of 1–3 km and less than 10% within the radius of 4–5 km are tentatively designated as rural stations, and nine rural stations are selected (Figure 1a). The geographic information of urban and rural stations are shown in Tables S3 and S4.

2.3.2. Indices and Calculation Methods

UHII was defined as the temperature difference between urban and suburban (rural) areas. The rural temperature (T_r) is the average value of the nine rural reference stations, while the urban temperature (T_u) is the average value of the urban stations in the central urban area of the Fourth Ring Road. Therefore, UHII (ΔT_{u-r}) can be obtained by the following formula (Yang et al., 2013):

$$\text{UHII} = \Delta T_{u-r} = T_u - T_r \quad (1)$$

In addition to daily mean UHII, UHII_{\max} , and UHII_{\min} were also calculated by applying Equation 1 for daily maximum temperature (T_{\max}) and daily minimum temperature (T_{\min}). Since T_{\max} often appears at about 14:00 LST and T_{\min} usually appears at late night or early morning near sunrise, the UHII_{\max} and UHII_{\min} were used to refer to the UHII at daytime and nighttime respectively.

Wind speed (WS), as an important indicator of wind field, is also an indispensable part of urban climatology, affecting UHI, air pollution, and surface hydrological processes (i.e., evapotranspiration) (Hou et al., 2013). Higher WS is helpful to the diffusion of atmospheric pollutants and UHI is usually weaker in windy days and seasons (Alonso et al., 2007). Low WS is thus conducive to the accumulation and storage of heat and pollutants. The difference between the rural and urban areas, which is defined as urban stilling island (USI), can be used to characterize the near-surface heat storage and exchange in urban and rural areas.

The USI intensity (USII) is defined herein as the WS difference between rural stations and urban stations. The rural WS (WS_r) and the urban WS (WS_u) denotes the mean 10 m WS of rural and urban station. Similarly, the USII (ΔWS_{r-u}) can be obtained by the formula (P. Yang et al., 2020):

Table 1
Distribution of Sample Size and Mean Value for Different Pollution Levels

		Mean value/sample size			
PM _{2.5} level ($\mu\text{g m}^{-3}$)		Whole year	Spring	Summer	Autumn
excellent	0–35	20.9/300	23.7/54	22.9/67	18.4/98
well	35–75	53.6/277	52.8/76	54.7/71	56.5/60
slight	75–115	91.9/140	92.6/47	88.4/33	91.7/33
moderate	115–150	129.1/51	131.9/15	127.7/1	123.4/18
severe	150–250	192.6/65	180.3/17	154.1/1	192.1/23
serious	>250	327.3/14	323.3/5	—	329.6/9

$$\text{USII} = \Delta\text{WS}_{\text{r-u}} = \text{WS}_{\text{r}} - \text{WS}_{\text{u}} \quad (2)$$

We first analyzed the distribution characteristics of PM_{2.5} concentration in the Beijing area. According to the hourly PM_{2.5} concentration data released in real-time, the daily average PM_{2.5} concentration of each monitoring station in Beijing is calculated. The daily time range is the same as the meteorological data. Because some monitoring stations are built around industrial sites on the outskirts of Beijing to monitor industrial emissions, cannot accurately characterize the concentration of regional pollutants. Therefore, according to the information in Table S2, the average value of all stations within the Sixth Ring Road are taken as Beijing's PM_{2.5} concentration and made use of in subsequent calculations and research.

Under the background of the ambient air quality standard of the people's Republic of China (GB3095–2012), PM_{2.5} concentration is divided into six different air quality levels. And on this basis, the influence of the PM_{2.5} concentration on UHII was studied. PM_{2.5} concentration samples under different levels are shown in Table 1.

Urban turbidity island (UTI), a phenomenon in which the turbidity in the urban area is significantly greater than that in the suburbs due to the difference in air quality between urban and rural areas, is an important topic of urban air pollution research (Zhou & Zheng, 1991). UTI was also called as urban pollution island (UPI) recently (Crutzen, 2004; Li et al., 2018, 2020). The difference between urban areas and suburban/rural areas was defined as the UTI/UPI intensity, in analogy with the UHII. Different from the calculation of UHII, in accordance with Table S2, we used urban environmental stations (PM_u) within the Fourth Ring Road and rural environmental stations (PM_r) to calculate the UTI intensity (UTII):

$$\text{UTII} = \Delta\text{PM}_{\text{u-r}} = \text{PM}_{\text{u}} - \text{PM}_{\text{r}} \quad (3)$$

The vertical temperature lapse rate (TLR) is a result of surface energy balance, which determines atmospheric stability above the surface (He & Wang, 2020; Holden & Rose, 2011; Qin et al., 2021). The TLR below 2 km altitude was also calculated here using L-band sounding data.

The boundary layer height (BLH) can be used to illustrate atmospheric stability. In this study, the potential temperature method is used to calculate the BLH. The detailed method can be obtained from Liu and Liang (2010).

Zhang et al. (2017) established the stable weather index (SWI) based on ten meteorological elements with strong indicative significance, which can well express the horizontal and vertical exchange capacity of regional atmosphere. The higher the SWI is, the weather system is more stable and the atmospheric exchange capacity is weaker. The SWI is also used in the following research.

2.3.3. Definition of Fine and Clear Weathers

Fine and clear weathers were defined herein. Weather condition is also an important factor affecting PM_{2.5} UHII relationship. In order to eliminate the weather condition effect, the weather process records of Beijing station are used to exclude the strong convective or unstable weather such as precipitation, snowfall, thunderstorm and sandstorm, and the relatively stable, fine weather such as clear-sky, cloudy condition, foggy, and haze weather was screened out. In particular, light or calm wind conditions were considered. As

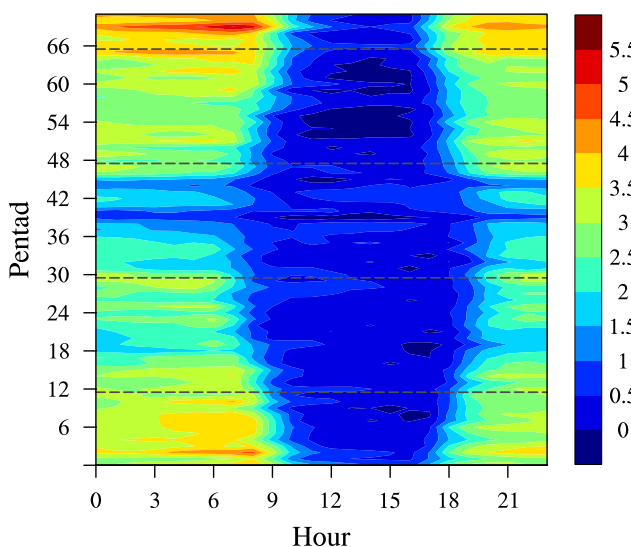


Figure 2. The hour-pentad plot of the urban heat island intensity averaged for the whole urban area for the time period 2016–2018. Dashed horizontal lines mark the boundaries of the four seasons.

which is the weakest UHII at nighttime among the four seasons, but the UHII of daytime in summer is the highest in the four seasons. At the end of summer, there is a high-value area of UHII in the daytime, and it lasts for a long time; in the middle of summer, the UHII is negative in part of the daytime. The extremely weak UHI may be caused by continuous rainfall which generated by daytime systemic weather. The diurnal variation of UHII within the summer is less than that of the other three seasons, and the intraday variation of UHII in winter and autumn is larger. The results of the hour-pentad plot of the UHII in Beijing are basically consistent with those of Yang et al. (2013).

Correspondingly, the average concentration of PM_{2.5} in urban areas varies greatly throughout the year (Figure S3). From the perspective of seasonal changes, the highest and second-highest PM_{2.5} concentrations appeared in spring and winter respectively, followed by autumn and summer. The PM_{2.5} concentrations and UHII values under fine and clear weather in the summer and winter of 2016–2018 are selected, and the every five days average is calculated. The result of the pentad change is shown in Figure 3. In summer, the two variables have opposite variations. It can be seen that when the PM_{2.5} concentration increases, UHI is often decreases correspondingly. After excluding the precipitation weather, the effect of precipitation that reduces PM_{2.5} concentrations and UHI at the same time has been eliminated, the reversed synchronous variation of the two appears. In winter, however, PM_{2.5} concentration and UHI is relatively consistent with each other. This result was particularly evident in 2016. In the winter of 2018, air quality has gradually improved, attributed to a series of environmental protection measures taken by local governments, and may also cause an asynchronous variation in PM_{2.5} and UHI in a short time period of February.

3.2. Association of PM_{2.5} and UHI

Figure 4 displays the correlation between daily PM_{2.5} concentration and UHII_{ave}, UHII_{max}, and UHII_{min} in Beijing under fine and clear weathers in winter and summer. In Figure 4a, the correlation between UHII_{ave} and PM_{2.5} concentration is positive in winter and negative in summer, and the correlation coefficients are 0.17 and -0.47, respectively. The increasing PM_{2.5} concentration tends to reduce the UHII_{ave} in summer but increase it in winter. This correlation pattern is the same as UHII_{max}. It can be seen that UHII_{max} is positively correlated with particulate with a correlation coefficient of 0.48 during winter daytime. However, there is a negative correlation between UHII_{max} and PM_{2.5} concentration in summer, which means that the lower aerosol concentration accompanies the higher UHII_{max}, and the correlation coefficient between the two is -0.18. UHII_{min} decreases with increasing aerosols in two seasons, with a lower correlation coefficient (-0.10) in winter but a high correlation coefficient (-0.41) in summer. The correlation of UHII_{min} with

many existing studies have shown, the UHII is dependent on wind speed and the UHII decreases as wind speed increases. At the same time high wind speed reduces PM_{2.5} concentration and results in correlation error. To avoid these, samples with daily averaged wind speeds $>3.3 \text{ m s}^{-1}$ were excluded on the basis of the Beaufort wind-force scale (Oke et al., 2017), the remaining samples were defined as fine and clear weathers.

Finally, under fine and clear weathers conditions, samples were reclassified. Sort the PM_{2.5} concentration values of samples in different seasons, and regard the top 50% of the samples as pollution days, otherwise as clean days. This reclassification will be used to compare the differences of parameters under different conditions.

3. Results

3.1. Characteristics of UHI and PM_{2.5} Variation

According to the hour-pentad plot of the UHII averaged for the whole urban area in Beijing (Figure 2), it can be seen that the UHII is strong in autumn and winter, especially at night, and lasts for a long time. The daytime UHI in winter is higher than that in autumn, and the phenomenon of the urban cold island can be observed in the daytime in autumn. The UHII at nighttime in spring and summer is weak, particularly in summer,

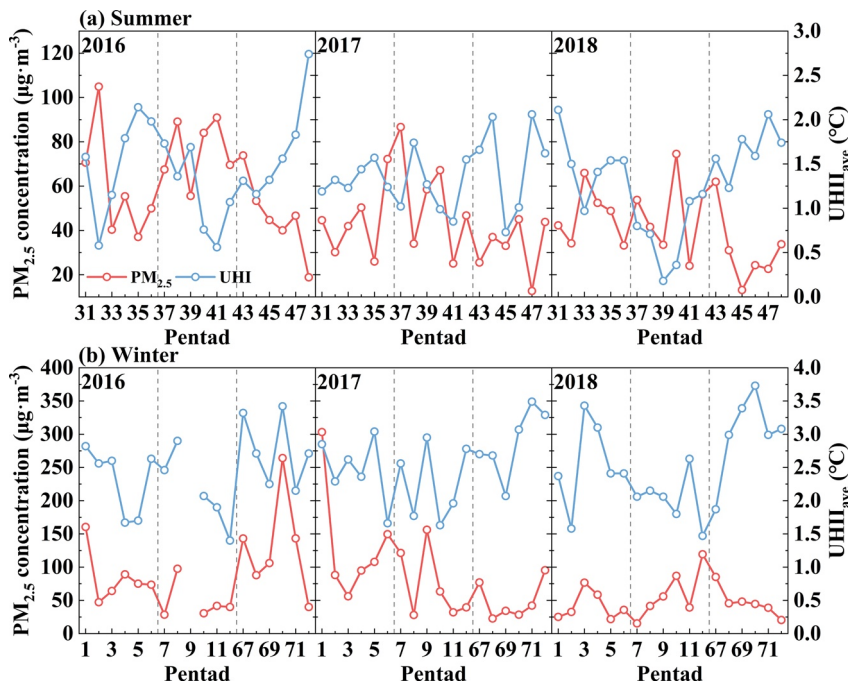


Figure 3. Time series of pentad PM_{2.5} concentration and urban heat island intensity (UHII)_{ave} at Beijing under fine and clear weathers in (a) summer and (b) winter of 2016–2018.

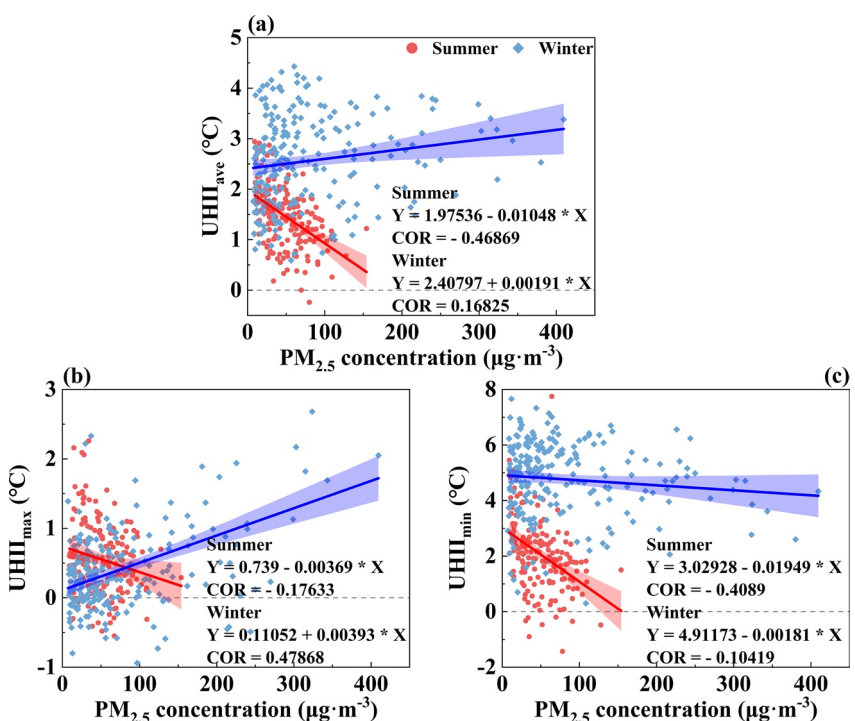


Figure 4. (a) Urban heat island intensity (UHII)_{ave}, (b) UHII_{max}, and (c) UHII_{min} as a function of PM_{2.5} concentration under fine and clear weathers. The red and blue lines are the linear best-fit line through the points, and shadows are the confidence intervals of the fitting lines, the two colors indicate summer and winter, separately. The least squares regression equation is given in each panel. The coefficient correlation (COR) is also given, and all of them are significant with $p < 0.05$.

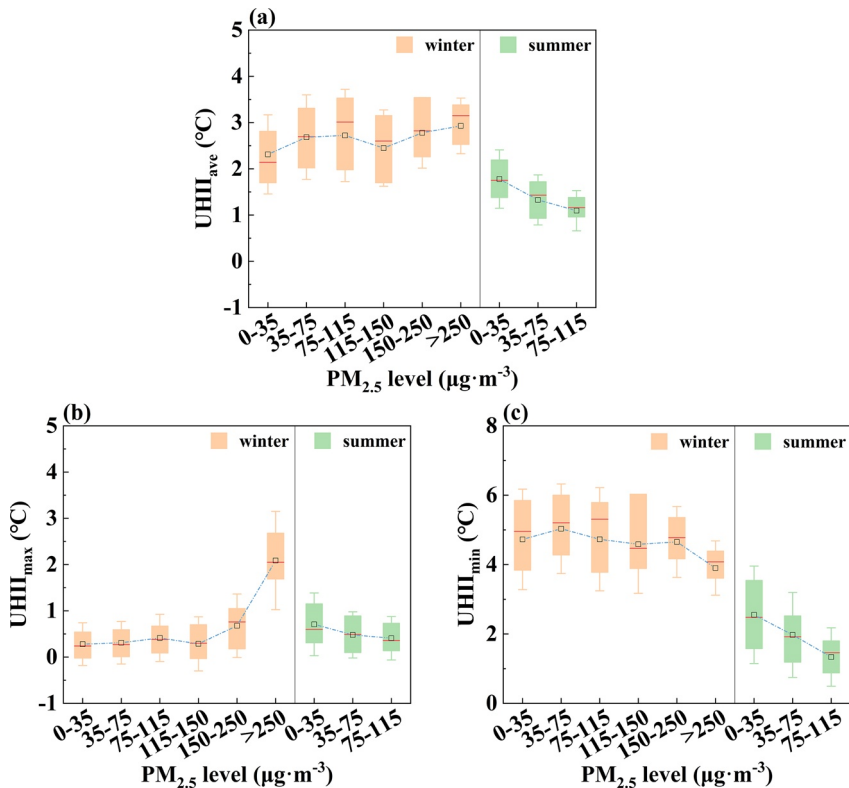


Figure 5. Distribution of urban heat island intensity (UHII_{ave} (a), UHII_{max} (b), and UHII_{min} (c)) as a function of $\text{PM}_{2.5}$ concentration level at Beijing under fine and clear weathers in winters and summers of 2016–2018. The hollow box is the average value, the red line is the median value, the boxchart value from the bottom to up is the mean value minus one time of standard deviation, 25% quantile line, 75% quantile line, the mean value plus one time of the standard deviation.

$\text{PM}_{2.5}$ concentration in winter may provide a different physical mechanism compare to the other two UHII conditions. The UHII_{max} change with aerosol in winter is very special in that it has a significant positive correlation with the aerosol level, and this also determines the same variation of the UHII_{ave} with aerosol.

The same method was used for the clean day and pollution day to study the relationship between $\text{PM}_{2.5}$ and UHII in different pollution concentration intervals. As shown in Figure S4, for UHII_{ave} and UHII_{max} , whether in summer or winter, the change of $\text{PM}_{2.5}$ concentration did not change its relationship with UHII. The effect of $\text{PM}_{2.5}$ on the UHII at different concentrations intervals consistently weakens UHII in summer and strengthens UHII in winter. The same is true for UHII_{min} in summer. However, $\text{PM}_{2.5}$ has opposite effects on UHII_{min} in winter at different intervals. UHII_{min} increases in the relatively clean condition but decreases in the polluted condition with $\text{PM}_{2.5}$ changes.

We further calculated and compared the variation ranges of UHII and their corresponding mean under different pollution levels under fine and clear weathers (Figure 5). The level standard was shown in Table 1. With the change of $\text{PM}_{2.5}$ concentration, UHII in different seasons has obvious changes. In winter, when Beijing's air quality changes from excellent to serious pollution, the average UHII_{max} increased from 0.28°C to 2.08°C , the UHII_{min} decreased from 4.72°C to 3.9°C , and the UHII_{ave} increased from 2.31 to 2.93°C . In summer, however, we observed a different pattern of the $\text{PM}_{2.5}$ –UHII relationship. Among the three pollution levels from excellent to slight, the average value of UHII_{ave} (UHII_{max} , UHII_{min}) changed from 1.78 ($0.71, 2.55$) $^{\circ}\text{C}$ to 1.09 ($0.41, 1.34$) $^{\circ}\text{C}$, showing an obvious downward trend with pollution level. When the air pollution in winter becomes more serious, the variation range of UHII_{max} under different pollution levels gradually increases while the variation range of UHII_{min} gradually decreases. Except for $\text{PM}_{2.5} > 250 \mu\text{g m}^{-3}$ situation UHII_{max} is less discrete than UHII_{min} . In summer the variation range of UHII also decreased during the polluted period, and the variation of UHII_{max} is much smaller than UHII_{min} obviously, which indicated

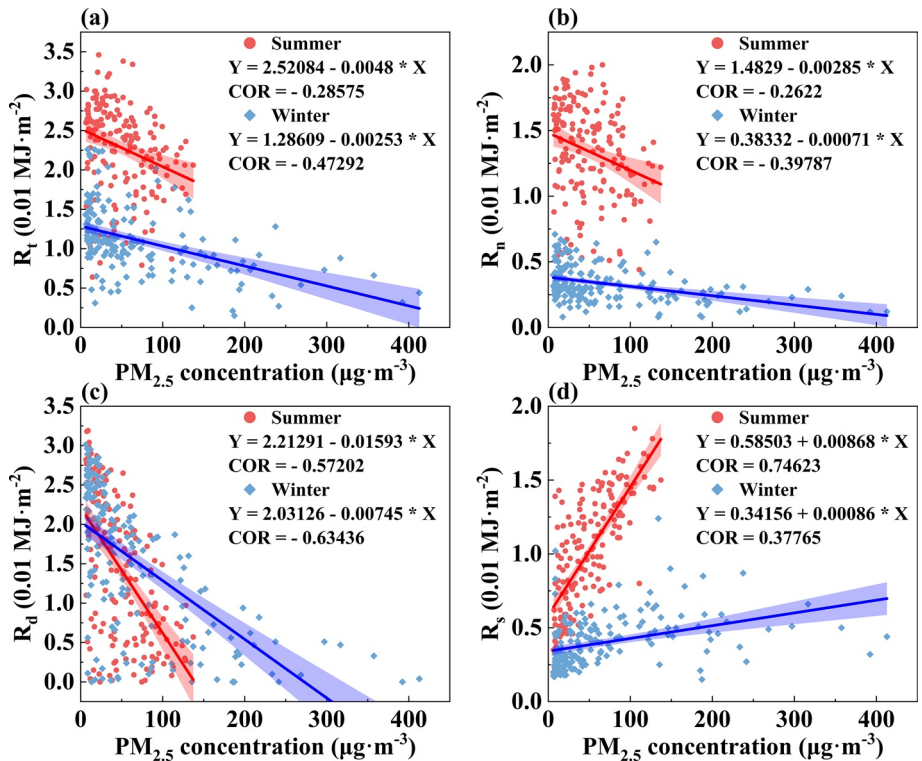


Figure 6. Relationship of the total (a), net (b), direct (c), and scattered (d) radiation with PM_{2.5} at daytime under fine and clear weathers in summer and winter of 2016–2018. All of them are significant with $p < 0.05$.

that the PM_{2.5} has a greater impact on UHII during daytime and this impact will increase with pollution. When the pollution level increases, these positive correlations are more significant in winter. These correspondences become more prominent in the case of heavy pollution, with the UHII_{max} rising sharply when the PM_{2.5} concentration level is greater than 250 $\mu\text{g m}^{-3}$.

3.3. Mechanism of Association of PM_{2.5} and UHII

3.3.1. PM_{2.5} and Radiation During Daytime

We analyzed the relationship between the daytime total radiation, net radiation, direct radiation, and scattered radiation and the daytime PM_{2.5} concentration under fine and clear weather, and the results are shown in Figure 6. The increase of particulate matter directly leads to the decrease of incident radiation and the increase of scattering radiation, which indicates that aerosol reduces the total surface radiation through absorption and scattering. For incident radiation, summer PM_{2.5} has a negative correlation on total, net, and direct radiation with correlation coefficients of -0.29, -0.26, and -0.57, respectively. This negative correlation is further enhanced in winter, with correlation coefficients reaching -0.47, -0.39, and -0.63. A winter-summer comparison of the correlation between PM_{2.5} and radiation (Figures 6a–6c) shows that the attenuation effect of aerosol on solar radiation in winter is stronger than that in summer. Figure 6d shows that the scattering and reflection effect of aerosol on solar radiation in summer is stronger than that in winter. The correlation between the scattering radiation and PM_{2.5} in summer (0.75) is much bigger than in winter (0.38). Therefore, compared with summer, winter particles with weaker scattering effect have stronger radiation attenuation ability, which means the absorption capacity of aerosol for radiation energy in winter is stronger, so as to heat the atmosphere and reduce the total solar radiation received by the surface.

3.3.2. Urban Turbidity Island and UHI During Daytime

As the pollution level rises, the urban-rural difference in particulate becomes more obvious (Figure S5). This difference is defined as the UTI. The uneven distribution of urban and rural particulate matter will

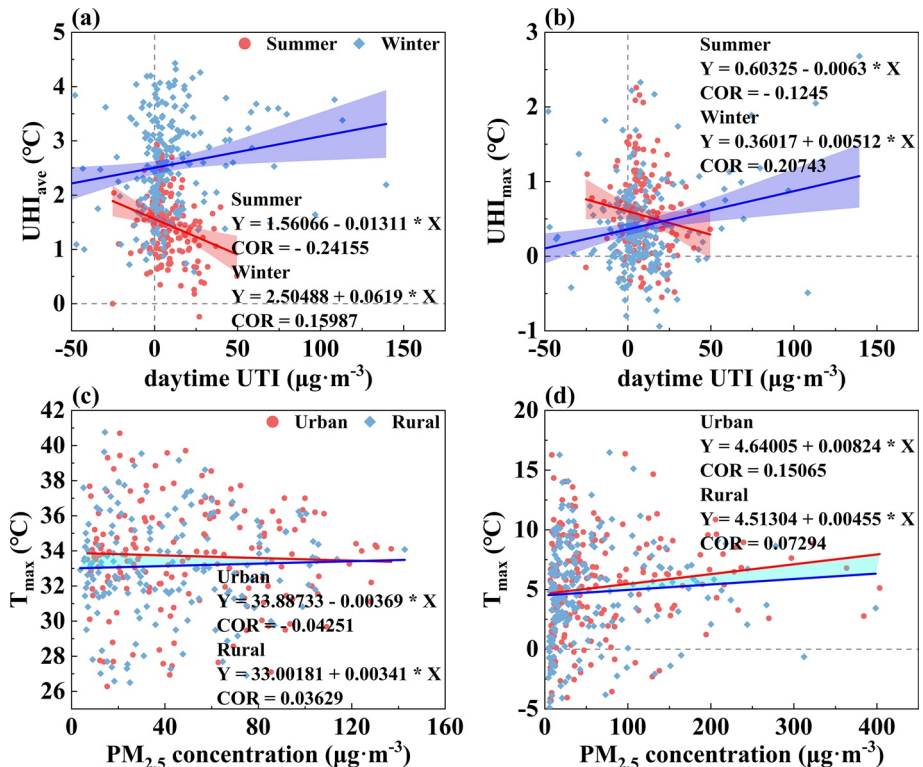


Figure 7. Relationship of the daytime Urban Turbidity Island intensity (UTII) with urban heat island intensity (UHII_{ave}) (a) and UHII_{max} (b) under fine and clear weathers in summer and winter of 2016–2018; Relationship between urban and rural daytime $\text{PM}_{2.5}$ and T_{max} in summer (c) and winter (d) of 2016–2018. All of them are significant with $p < 0.05$ except for (c).

directly affect the acceptance of radiant energy in urban and rural areas, and indirectly affect the changes in urban and rural air temperature, thereby changing the urban heat island. The relationship between daytime UTII and daily UHII (UHII_{ave}) is shown in Figure 7a. There is an opposite correlation in two seasons, with a negative correlation coefficient of -0.24 in summer and a positive correlation coefficient of 0.16 in winter. Since the incident radiation has a more direct impact on the temperature during the daytime, the correlation between daytime UTII and daytime UHII (UHII_{max}) can better show the impact of particles on the UHII, as shown in Figure 7b. In summer daytime, high UTII caused a decrease in UHII_{max} , with a correlation coefficient of -0.12. In contrast, in the winter daytime, UTII and UHII_{max} show a positive correlation with a correlation coefficient of 0.21. The effect of daytime UTII on UHII is the same as that of Figure 4. Figures 7c and 7d shows the impact of $\text{PM}_{2.5}$ in urban and rural areas on regional T_{max} during daytime. In summer, $\text{PM}_{2.5}$ in urban areas and rural areas respectively make the temperature decrease and increase, which reduces the temperature difference between urban and rural areas and weakens the UHII. In winter, both urban and rural $\text{PM}_{2.5}$ causes the temperature to rise, but the upward trend in urban is higher than that in rural, which increases the temperature difference and strengthens UHII.

Through analysis of ERA5-Land radiation data set, we have obtained the net total radiation of urban and rural stations. Similarly, by analyzing the correlation between $\text{PM}_{2.5}$ and net radiation in urban and rural areas during daytime (Figures S6a and S6b), it can be shown that the effect of $\text{PM}_{2.5}$ on net radiation is very similar to that on the temperature, with $\text{PM}_{2.5}$ decreasing net radiation in urban areas but increasing it in rural areas slightly in summer. In winter, however, there is a consistent downward trend, and the decrease in urban areas is slightly stronger. The differential distribution of particles in urban and rural areas and its impact on the radiation balance may be one of the direct reasons for the changes in the UHII caused by $\text{PM}_{2.5}$ concentration.

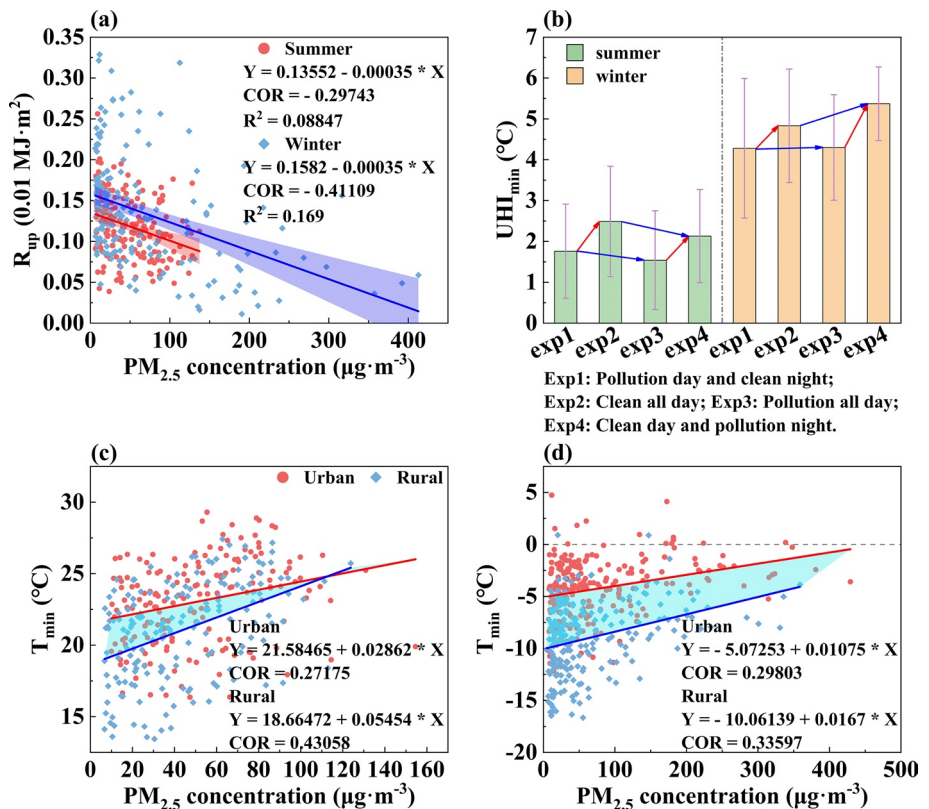


Figure 8. (a) Relationship of the upward radiation at nighttime with PM_{2.5} at daytime under fine and clear weathers in summer and winter of 2016–2018; (b) Changes of urban heat island intensity ($UHII_{min}$) at night under four different experimental conditions. The red and blue arrows indicate the $UHII_{min}$ changes caused by the changes in PM_{2.5} from clean to pollution during the day and night, respectively. Relationship between urban and rural daily PM_{2.5} and T_{min} in summer (c) and winter (d) of 2016–2018. All of them are significant with $p < 0.05$.

3.3.3. Daytime PM_{2.5}, UHII_{min} and Nighttime Upward Long-Wave Radiation

Figure 8a shows the correlation between daytime PM_{2.5} concentration and nighttime upward radiation. Both of them show a negative correlation in winter and summer, with the correlation coefficients of -0.41 and -0.30, respectively. When the daytime particles weaken the incident radiation, and indirectly reduce the radiation energy received and stored on the ground, the upward radiation at night decreases accordingly. Since the particles attenuation effect on incident radiation is stronger in winter and daytime PM_{2.5} concentration has a greater impact on the nighttime upward radiation in winter.

In order to examine the effect of varied pollution levels in different time on nighttime UHII, we design the following four sets of experiments and calculate the means $UHII_{min}$ for different experiments. And the requirements and results are shown in Figure 8b. Through comparing different experiments to understand the impact of changes in PM_{2.5} concentration in different time periods on $UHII_{min}$ at night. In summer, comparing exp1 and exp2 or exp3 and exp4 to find that no matter whether the night is clean or not, when the daytime is clean, the $UHII_{min}$ at night is higher. More daytime pollutants result in lower night UHII. In winter, this phenomenon is equally obvious. In addition, comparing exp1 and exp3 or exp2 and exp4 in different seasons, the opposite effect of PM_{2.5} concentration changes at night on $UHII_{min}$ in summer and winter can be observed. Nighttime pollutants weaken the $UHII_{min}$ in summer but strengthen it in winter. Under the condition that the daytime is clean in winter, the $UHII_{min}$ rises significantly with the increase of nighttime aerosol level, probably indicating that winter aerosol has an obvious thermal insulation effect at night and benefits the increase of the nighttime UHII.

Therefore, the radiation response to aerosols can be divided into two aspects: cooling effect (i.e., daytime aerosol reduces the radiation reaching the ground via absorbing and scattering solar short-wave radiation,

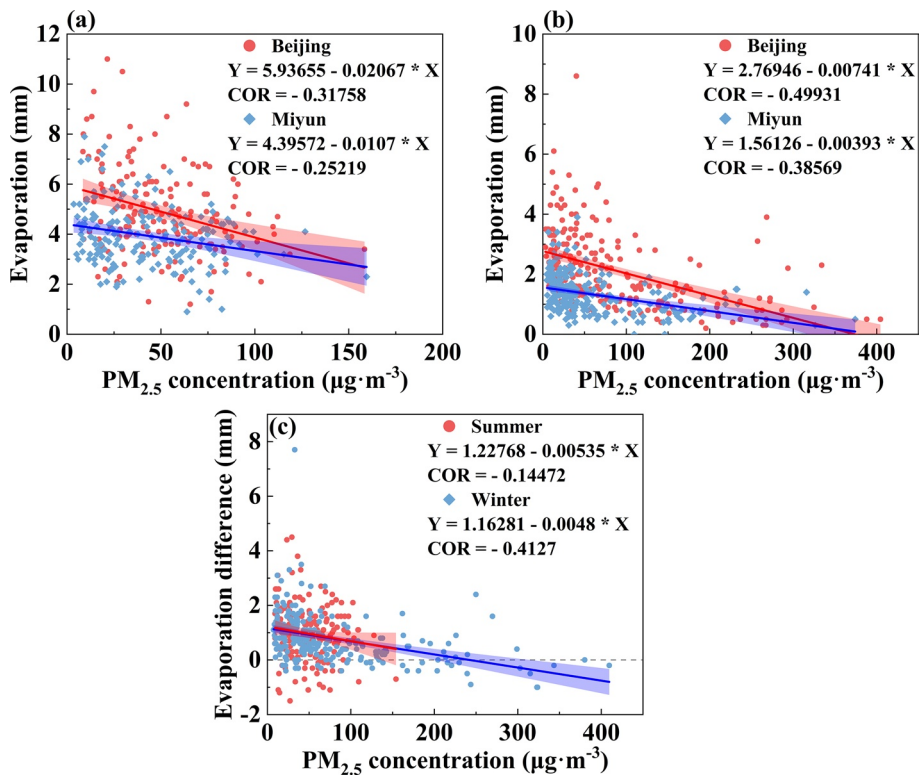


Figure 9. Relationship of daily evaporation with PM_{2.5} under fine and clear weathers in summer (a) and winter (b). (c) Relationship of the daily evaporation difference between Beijing and Miyun stations with PM_{2.5} of 2016–2018. All of them are significant with $p < 0.05$.

and the surface temperature and surface air temperature at night are relatively lower) and warming effect (i.e., nighttime aerosols emit atmosphere long-wave radiation downward, and the surface temperature and surface air temperature rises relatively). In general, the combined effect of aerosols will increase the T_{\min} at night. The above results of the T_{\min} (Figures 8c and 8d) indicate that, whether in summer or winter, PM_{2.5} will increase the temperature at night in rural areas faster than in urban areas and reduce the temperature difference between urban and rural areas, leading to the weakening of UHII. The daily PM_{2.5} concentration shows the same effect on the daily net total radiation (Figures S6c and S6d), which reduces the radiant energy difference between urban and rural areas and alters temperature. Compared with winter, the reduction of temperature difference in summer with the change of PM_{2.5} concentration is more obvious, which is similar to the result shown in Figure 4c.

3.3.4. Daily PM_{2.5} and Evaporation

Pan-evaporation can represent the evaporation capacity of an area. Figure 9 shows the effects of daily PM_{2.5} on evaporation in two observational sites of Beijing and Miyun, which represent urban and rural areas respectively. PM_{2.5} reduces pan-evaporation in both summer and winter. Beijing and Miyun stations show negative correlations of -0.32 and -0.25 in summer and -0.50 and -0.39 in winter, respectively. PM_{2.5} has a higher impact on evaporation in urban areas, which is related to the larger reduction of solar radiation by aerosols. Therefore, with the increase of PM_{2.5}, the difference in pan-evaporation between urban and rural areas has gradually decreased. Figure 9c shows the effect of average PM_{2.5} on pan-evaporation differences between urban and suburban stations. PM_{2.5} is negatively correlated with the difference in the urban-rural pan-evaporation, and the correlation coefficients are -0.14 and -0.41 in summer and winter, respectively. The more significant reduction in pan-evaporation difference with PM_{2.5} in winter means that the increase in aerosols has a relatively weaker impact on rural evaporation, which may compensate for the reduced evaporation in rural areas due to radiation reduction.

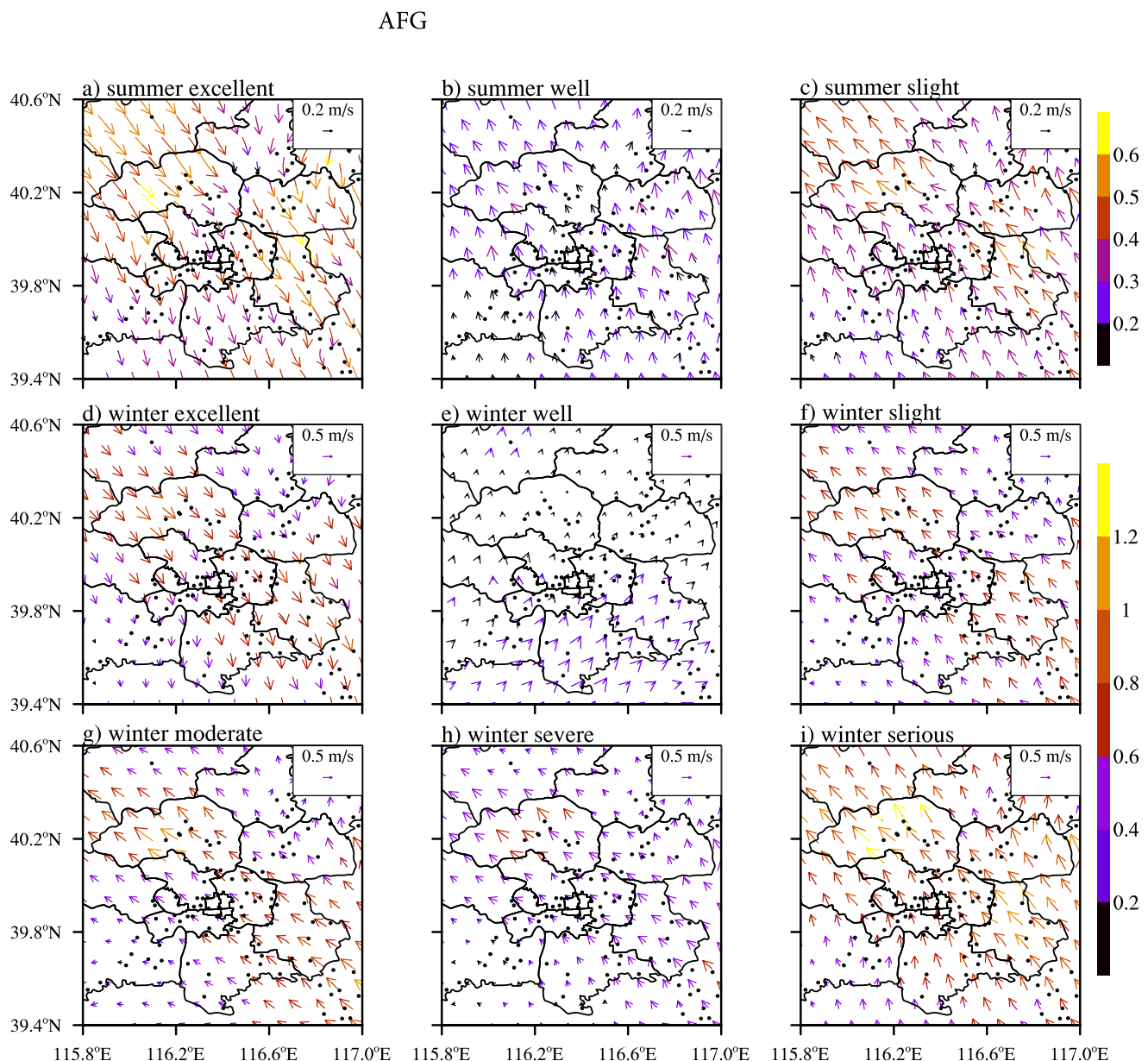


Figure 10. Average wind anomalies under different pollution levels in summer (a–c) and winter (d–i). The different pollution levels and their PM_{2.5} concentration range are shown in Table 1. Black dots represent wind observation stations with quality-control.

3.3.5. Horizontal Wind Speed Under Different Pollution Conditions and UHII

Figure 10 shows wind field anomalies in Beijing under different pollution levels (Table 1). When the air quality is excellent, Beijing usually has a strong northwesterly wind anomaly. Considering the background wind field (Figure S7), the southerly winds weaken in summer and the northerly winds increase in winter under excellent air conditions. As the pollution level increases, the background wind field changes from northerly to southerly wind anomalies. The pollution accompanies the intensified southerly wind and the weakened northerly wind in summer and winter, respectively. This maybe one of the reasons why the impact of PM_{2.5} on UHII in different seasons is opposite. Wind will affect the diffusion of pollutants and the UHI intensity at the same time. Beijing's pollution sources appear in industrial areas or cities (e.g., Baoding, Langfang, and Shijiazhuang cities) south of Beijing. In summer, the southerly wind prevails. When the southerly wind speed increases, the pollutants are blown to the urban area of Beijing, causing the pollution level to rise. At the same time, the increased wind speed increases the heat diffusion between urban and

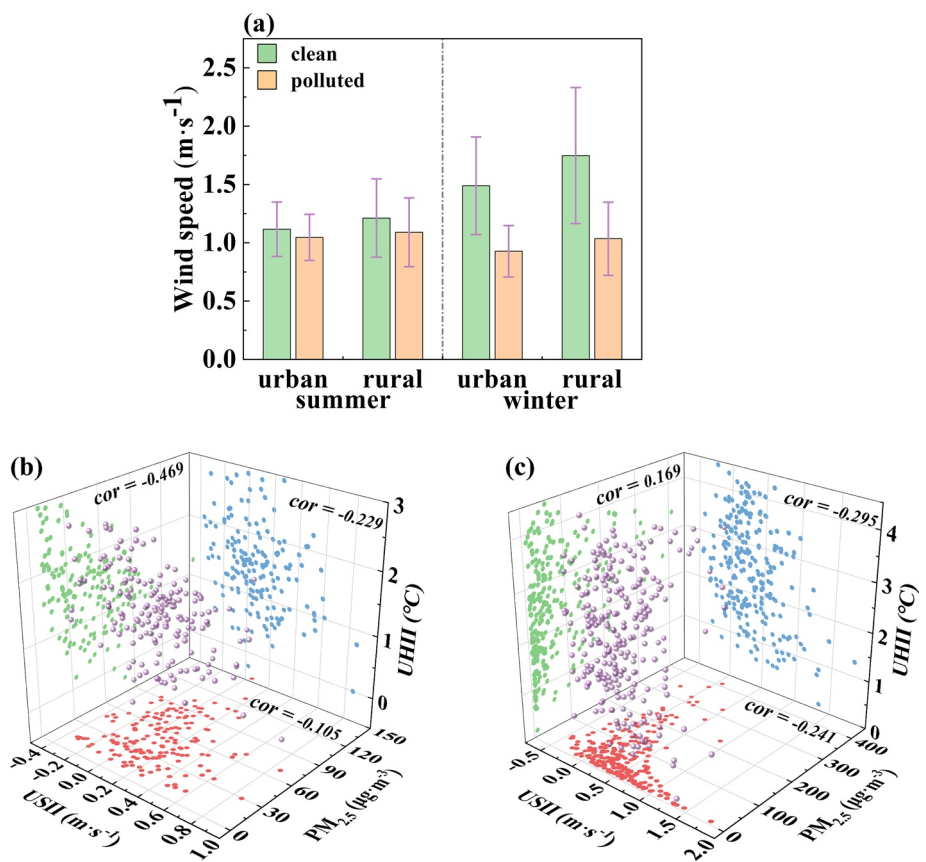


Figure 11. (a) Comparison of average wind speeds (unit: m s⁻¹) between urban and rural areas under clean and polluted conditions in summer and winter. Relationship of the daily PM_{2.5} concentration, urban stilling island intensity (USII) and urban heat island intensity (UHII) under fine and clear weathers in (b) summer and (c) winter of 2016–2018. All of them are significant with $p < 0.05$ except summer in (a).

rural areas and reduces the UHII. In winter, the northerly wind prevails and often brings pollutants to the more southern areas, making Beijing cleaner. The positive southerly wind anomalies make it difficult for pollutants and heat to diffuse, resulting in increased pollution and UHII. During severe pollution events in winter, the positive southerly wind anomaly reaches its maximum, and the overall average wind field shows an obvious weak warm advection from the south (Figure S8).

The average urban and rural wind speed on polluted and clean days in summer and winter is calculated and shown in Figure 11a. As expected, whether in urban or in rural, the seasonal mean wind speed in winter is higher than in summer under clean conditions, the transfer of heat will also be more convenient. The wind speed in rural areas is higher than that in urban areas, and the urban-rural difference in average wind speed is higher in winter than in summer. As the air quality deteriorates, the average wind speed is lower under polluted conditions than that under clean conditions, especially in winter when the wind speed in urban areas decreases by 0.56 m s⁻¹ and that in rural areas by 0.71 m s⁻¹. In summer, however, the decrease of wind speed in urban and rural areas is not obvious as the pollution worsens, are only 0.07 m s⁻¹ and 0.12 m s⁻¹ respectively. The urban-rural difference in average wind speed has also changed, dropping by 0.15 m s⁻¹ in winter and 0.05 m s⁻¹ in summer.

USI, defined as wind speed difference between rural and urban, can well describe the heat exchange between the city and its surroundings. Figure 11 also shows the relationship between daily USII and PM_{2.5} concentration, UHII_{ave}. By observing the distribution range of USII, it is not difficult to find that USII in winter is higher than in summer, which proves that the relative heat exchange between urban and rural areas in winter is higher. PM_{2.5} is negatively correlated with USII, and this phenomenon is more significant in winter, with a correlation coefficient of -0.24, indicating that a smaller wind speed contrast between

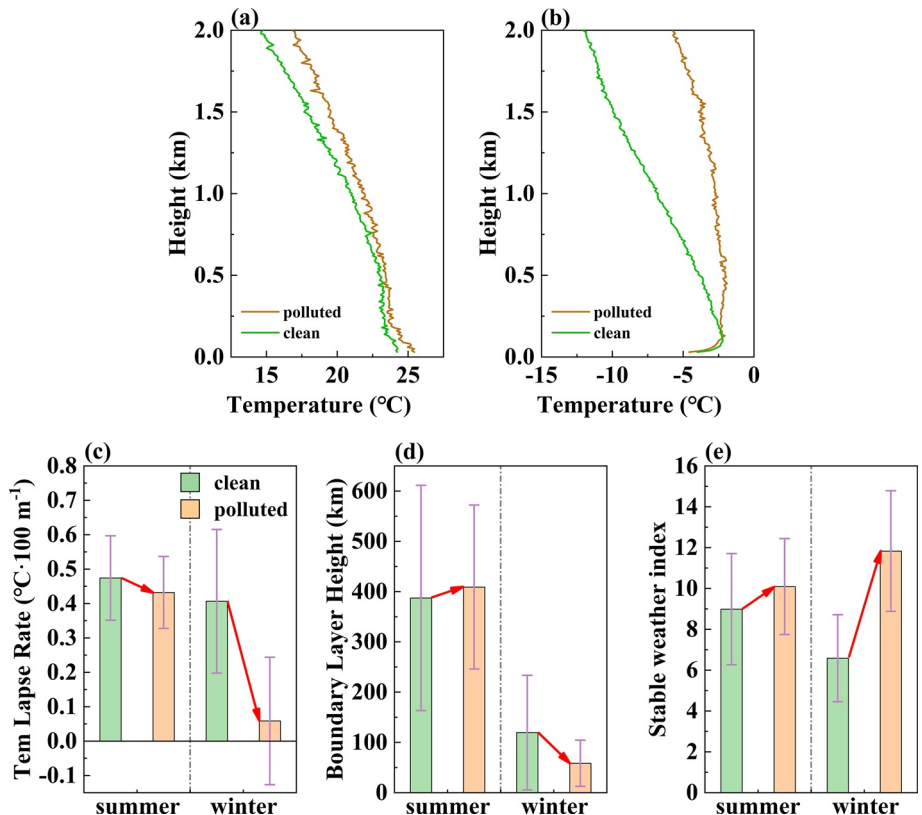


Figure 12. Summer (a) and winter (b) mean vertical temperature profiles under clean and polluted conditions. Average temperature lapse rate below 2.0 km (c), boundary layer height (d) and stable weather index (e) in summer and winter. The red arrows show the change ranges from clean conditions to polluted conditions. All of winter are significant with $p < 0.05$.

rural and urban areas under the background of weak wind field benefits the rise of $\text{PM}_{2.5}$ level in winter. On the other hand, $\text{PM}_{2.5}$ also affects the horizontal wind speed, more particles indirectly led to the weakening USII. There is a negative correlation between USII and UHII_{ave} , and the correlation coefficient is -0.23 in summer and -0.30 in winter. Heat is transferred between urban and rural areas through the difference in wind speed, thereby alleviating the urban heat island. The stronger the USII, the stronger the heat exchange between urban and rural areas, and the lower the UHII. $\text{PM}_{2.5}$ may also affect UHII through USII.

3.3.6. Atmospheric Stability, Pollution Conditions and UHII

Figure 12 shows the vertical temperature profiles in summer and winter in Beijing under pollution and clean conditions. The overall temperature in the polluted conditions in the profile is higher than that in the clean conditions. The vertical temperature gradient of polluted days is weaker than that of clean days, this is more prominent in winter. Due to the stronger radiation absorption capacity of winter aerosols, aerosols heat the atmosphere to increase the temperature and produce thermal inversion layer. Through these, aerosols reduce the vertical temperature gradient or TLR, which influences the stability, convection, and vertical heat exchange of atmosphere. Pollution in winter thus significantly weakens the TLR in lower troposphere, and generally increases atmospheric stability, which helps strengthen the UHII. However, because of the stronger scattering properties, the effect of summer aerosols on TLR and UHII is not so obvious.

Similar to the TLR, the BLH and the SWI are two other variables that can affect or describe the stability of the atmosphere. Their comparison under different pollution conditions in winter and summer are shown. In winter, aerosols significantly reduce the TLR, which confirms the above results. The average BLH in winter is much lower than that in summer, so the influence of BLH is more prominent in winter. When winter pollution occurs, BLH decreases sharply, with more stable atmospheric stratification. The SWI of polluted days in winter is much higher than that in clean days, however, the changes in the above indices caused by

polluted days and clean days are not obvious in summer. This can also prove that the atmospheric state in winter is more stable under polluted conditions. The more stable weather and the lower BLH will inhibit the exchange and diffusion of the heat in the urban canopy and boundary layer, contributing to a stronger UHII in winter.

4. Discussion

In this study, we analyzed the association of aerosols with the UHII. The association of summer and winter seems opposite. In winter, aerosol, together with other factors, may have strengthened the UHII. In summer, $PM_{2.5}$ may have weakened the UHII. The opposite results of $PM_{2.5}$ influence on annual mean UHII have been reported in previous studies. Through the studies for Thessaloniki and Beijing, the direct correlation between higher UHII and poor air quality has been discovered (Li et al., 2007; Poupkou et al., 2011) and further confirmed by modeling (Chen et al., 2018). Simulations indicate that this link may have been related to the higher absorbing and scattering of solar radiation by aerosols on polluted days. Chen et al. (2003) and Sang et al. (2000) also pointed out that the aerosol alters the UHII by influencing the radiation process. The difference is that they found that this process will reduce the UHII. Wu et al. (2017) proved that aerosols weaken UHII through the analysis of Nanjing, but this mainly occurs in summer. In their researches, aerosols have a greater impact on UHII during daytimes. Zheng et al. (2018) found that the difference in aerosol between urban and rural areas would increase the UHII in Beijing, while Li et al. (2018) suggested that this urban-rural difference would reduce UHII in Berlin. In their researches, aerosols have a greater impact on UHII at night.

In the study, we found different results from the previous ones. During the day, the daily aerosol weakens the UHII in the summer but strengthens it in winter. Through satellite data and model simulations, Han et al. (2020) reached conclusions similar to those in this study. Jin et al. (2010) found that aerosols have a weakening effect on surface and air UHII during summer daytime in Beijing and New York. However, regarding the UHII during winter daytime, the existing studies still have different opinions. Sang et al. (2000) and Y. Yang et al. (2020) showed that aerosols cause the decline of UHII during winter daytime. Wu et al. (2017, 2021) also found that aerosols slightly weakens daytime UHII in winter, although their conclusions were consistent with ours in summer. This opposite cognition may be related to different observational data. Only a small number of weather and environmental stations are used in the previous researches. In this study, a large number of observational stations with richer and more precise sample size and a finer spatial distribution are used.

Different results also appeared in the studies of UHII in winter night. Nighttime air UHII showed positive correlation with particles levels (Jonsson et al., 2004; Y. Yang et al., 2020; Zhang et al., 2004). Cao et al. (2016) estimated that the contribution of nighttime aerosol pollution to surface UHII is positive. In this study, however, we found that aerosols are negatively correlated with air UHII. The aerosols slow down the development of UHI at night. The previous studies paid more attention to the impact of nighttime aerosols on UHII at night, but this research is more concerned about the impact of the overall particle concentration within a day on UHII at different times. Therefore, our results show a more comprehensive impact of daily aerosols on the nighttime UHII. Although in Figure 8b we also observe the positive contribution of nighttime aerosol changes to nighttime UHII, we believe that daytime aerosols may have a stronger effect on nighttime UHII, thus showing the phenomenon that overall aerosols weaken nighttime UHII. This does not contradict the previous works. Analysis for different concentration intervals shows that $UHII_{min}$ increases in a relatively clean condition but decreases in a polluted condition. We infer that this may have been caused by the comprehensive impact of $PM_{2.5}$ on radiation, with the influence of daytime aerosol on nighttime UHII gradually strengthened. In the following paragraphs, the possible mechanism of aerosols causing temperature and UHII changes will be analyzed.

Y. Yang et al. (2020) considered that the influence of atmospheric particles on urban climate is mainly determined by direct and indirect ways, known as aerosol-radiation interaction and aerosol-cloud interaction, respectively. Here another indirect effect of aerosol will be introduced, namely aerosol-PBL interaction. Particles have a direct impact on climate by scattering or absorbing solar radiation. Scattering aerosols can reflect more solar radiation back into space, reduce the surface incident radiation, and cool the surface

(Huang et al., 2014; Huebert, 2003; Ramanathan et al., 2001; Rasch et al., 2001). The aerosol difference between urban and rural areas will reduce more solar radiation in urban areas, thereby reducing the temperature difference between urban and rural areas and weakening the urban heat island. Absorbing aerosols also change the radiation budget. The difference is that absorbing aerosols absorb solar radiation to reduce incident radiation on the surface, but this process heats the atmosphere and warms the near-surface (Jones et al., 2011), thereby enhancing the heat island. In addition, absorbing aerosols, by heating the atmosphere, reduce the vertical temperature gradient between the surface and the atmosphere, and make the atmospheric boundary layer tend to be stable. The stable atmosphere can further inhibit the diffusion of pollutants, thus producing a positive feedback (Ding et al., 2016; Gu et al., 2010; Huang et al., 2018; Li et al., 2017). This process is conducive to both heat accumulation and storage. No matter what property of aerosol, after intervening in the daytime radiation, is usually accompanied by a decrease in the radiant energy stored on the ground, and this part of energy is released in the form of upward radiation at night, affecting the urban climate.

The aerosol radiation effect can directly influence UHI. The increase in atmospheric stability caused by aerosols will also affect UHI, which can be called the indirect effect of aerosol. In addition, there is another aerosols indirect effect, that is, aerosols can also alter local surface and air temperature through the evaporative pathway (Bright et al., 2017). Aerosols alter the proportion of diffuse radiation in global solar radiation reaching the Earth's surface (Wang et al., 2008), and diffuse radiation results in higher light use efficiencies by plant canopies, which enhances transpiration and may alter the temperature (Gu et al., 2002). Aerosols increase the terrestrial evaporative fraction, or the portion of net incoming energy consumed by evaporation (Chakraborty, Lee, & Lawrence, 2021). When the local surface available energy changes little, the cooling via evapotranspiration of the surface vegetation in rural areas will also increase the UHII (Chakraborty, Sarangi, & Lee, 2021). However, although the aerosol increases the diffuse radiation, the total radiation decreases, which is closely related to the total evaporation. Aerosol radiative forcing reduces latent and sensible heat fluxes by 14% and 16% respectively. Less reduction in latent heat flux is attributable to increased evapotranspiration due to diffuse radiation-enhanced-photosynthesis (Murthy et al., 2014). In general, aerosols will reduce total evaporation and indirectly affect temperature.

4.1. Aerosol Direct Effect (Aerosol-Radiation Interaction)

To explore the effects of aerosol-radiation interaction, we examine the relationship of aerosols and radiations (Figures 6 and 7). During the summer daytime, particles have strong scattering characteristics of radiation, which reduces the incident radiation and lowering temperature (Figure 6). At this time, the difference in the spatial distribution of pollutants is particularly important for UHII changes. The difference in the average urban and rural particle concentration (also called the UTI) under different pollution levels is shown in Figure S5. With the increase of pollution, the spatial difference in air pollution between urban and rural areas has increased, the concentration of particulate matter in urban areas is higher than that in rural areas (Figure S4). Because of the different aerosol loads and properties between urban and rural areas, urban land surface experiences a larger reduction of solar radiation than rural land surface, affecting the surface/building absorption and the transmission of energy and the rise of surface air temperature in urban areas. The above process reduces the air temperature difference between urban and rural areas, thus reducing UHII. Then analyze the relationship between UTII and UHII, when the summer urban-rural PM_{2.5} concentration difference (UTII) increases, the UHII decreases (see Figure 7). We calculated the correlation of summer PM_{2.5} to temperature in urban and rural areas. As expected, particles have caused a decrease in urban temperatures and an increase in rural temperatures. Although the correlation is not significant, the summer PM_{2.5} will still weaken UHII. A similar situation is the impact of PM_{2.5} on radiation (Figures S6a and S6b), which further proves that aerosols can affect UHII by affecting radiation transmission through urban-rural differences. Wu et al. (2017) pointed out that daytime UHII reduction was strongest in July as both the PM_{2.5} concentration differences between the urban and suburban areas and the incoming solar radiation varied across different seasons. Since the incident solar radiation reaches its strongest in summer, it is more sensitive to aerosol weakening UHII. Figure 13a explains the process of how aerosols affect UHII in summer, and this process usually has a negative effect on UHII, which can be regarded as the direct effect of aerosol.

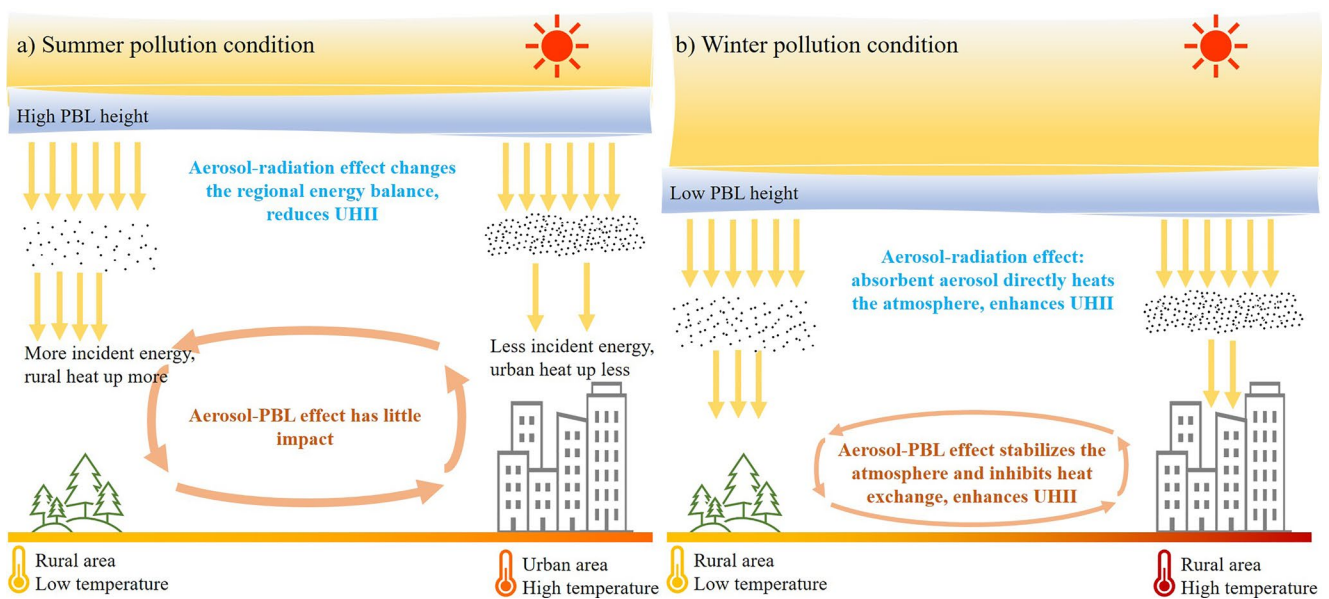


Figure 13. Schematic diagram of the process of aerosols affecting urban heat island (UHI) during daytime in different seasons: (a) summer and (b) winter pollution condition.

In winter, both urban and rural pollution is very serious, though the pollution level is still higher in urban areas. Likewise, the difference of particulate matter between urban and rural areas in winter are reinforced with particle pollution (see Figure S5). Unlike summer scattering aerosols, winter aerosols show stronger radiation absorption characteristics (see Figure 6). Aerosols directly warm the surface atmosphere by absorbing radiation. The PM_{2.5} concentration differences make the atmosphere in urban areas warmer than rural areas, and the pollutant dome above the urban area will also reduce the dissipation of long-wave radiation on the ground. The response of urban and rural temperature to PM_{2.5} shows that pollutants in the urban area make the temperature rise faster and the end result is an enhanced UHII (Figure 7). This process can be regarded as one of the reasons why aerosols make the UHII rise during the winter daytime and displayed in Figure 13b.

At night, due to the lack of solar radiation warming, the change of urban heat island is mainly caused by the atmospheric energy stored in the ground and urban canopy during the daytime and anthropogenic heat release, which heats atmosphere in the way of upward radiation, resulting in the temperature difference between urban and rural areas. On account of the increase of aerosol concentration in the daytime, the solar radiation reaching the surface decreases (Figure 6), the energy stored in the urban canopy and ground is reduced. Figure 8a displays the negative correlation between daytime aerosols and nighttime upward radiation. When the energy released through the ground upward radiation at night is reduced, and the air temperature of the city and the surrounding is relatively lower. Compared with rural areas, urban surfaces have a low thermal capacity, so their temperatures are thus more sensitive, resulting in a greater drop in temperature in urban areas and weakening nighttime UHII. The results of the four sets of experiments prove that, when the daytime is clean and the surface receives more radiant energy, the UHII_{min} at night is often higher than the UHII_{min} when the daytime is a polluted day (see Figure 8b). In the meantime, with the aggravation of nighttime pollution in winter, the difference between urban and rural PM_{2.5} concentration or UTII also increases, and the higher PM_{2.5} concentration in urban area increases the downward atmospheric long-wave radiation, which reduces the escape of heat within the urban canopy and is conducive to the increase in UHII. The attenuation (cooling) effect of daytime aerosols and the enhancement (warming) effect of nighttime aerosols conjunctively alter the nighttime UHII, and the dominant impact will vary with the concentration and composition of PM_{2.5}. In Figure S4f, under clean conditions, the ground receives and stores more radiant energy, and the warming effect of aerosols is stronger than the cooling effect, so the UHII_{min} shows an upward trend. However, under polluted conditions, aerosols will greatly weaken the incident solar radiation during the day, and the cooling effect of aerosols is larger than the warming effect,

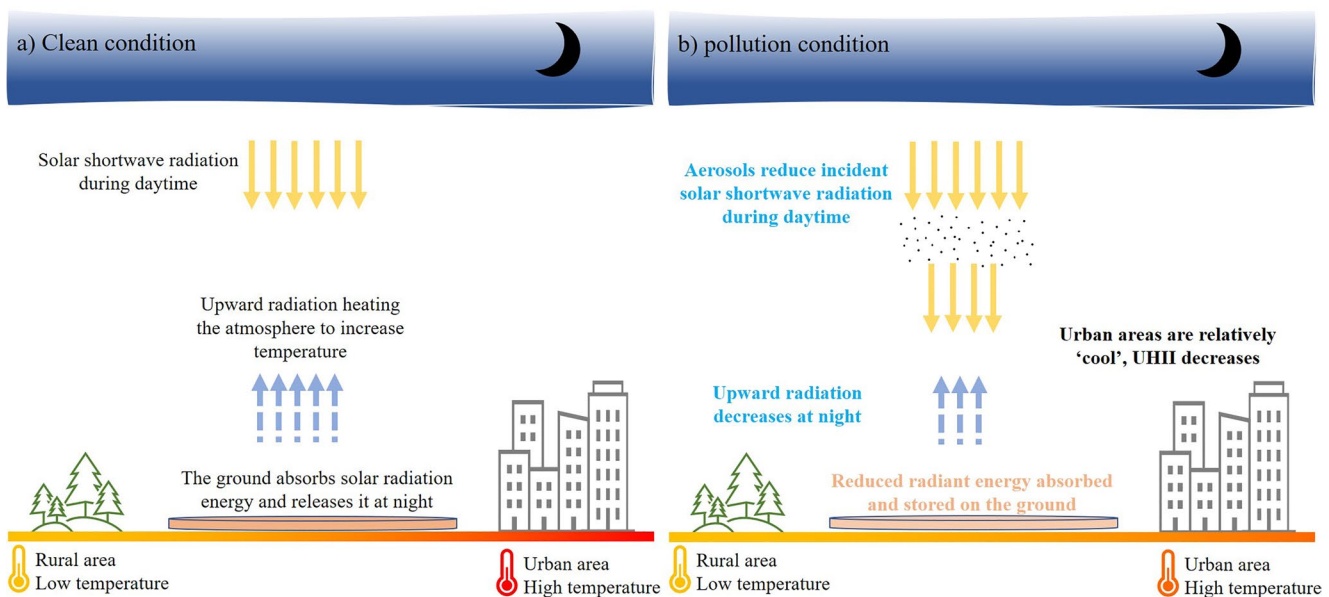


Figure 14. Schematic diagram of the process of aerosols affecting urban heat island (UHI) at night in different seasons: (a) clean condition, (b) pollution condition.

which will weaken the $UHII_{min}$. Compared with summer, the emission of absorptive aerosol in winter strengthens the warming effect, while the warming effect in summer is generally smaller than the cooling effect. Overall, the attenuation effect of daytime aerosols is higher than the enhancement effect of nighttime aerosols, which allows rural to receive more net radiation and makes the surface air temperature rise faster, resulting in a declining $UHII$. Figure 14 illustrates how daytime aerosols affect urban heat island at night.

4.2. Aerosol Indirect Effect (Aerosol-PBL Interaction)

In addition to the possible enhancement of the winter $UHII$, as the emission of absorbing aerosol increases in winter, it directly heats the atmosphere by absorbing solar radiation, leading to a smaller TLR or even a temperature inversion, a more stable air in the boundary layer, and a lower and shallower BLH, which inhibits the horizontal and vertical airflow and heat flux exchange between urban and rural areas. These, combined with other factors such as latitude, geomorphology and large-scale field of circulation, will enhance the $UHII$.

High pollution level can reduce near-surface wind speed. In Figure 11a, the urban and rural wind speeds under polluted conditions have been reduced. Among them, pollution occurs due to low wind speeds, but low wind speeds caused by high pollutants also exist, and the two form a positive feedback. Regardless of the wind direction, high wind speed is conducive to urban and rural heat exchange and can reduce $UHII$. On the contrary, low wind speed reduces the heat exchange between urban and rural areas, and the urban canopy can store more heat, increasing the temperature of urban areas and the $UHII$. Analyzing the association of $PM_{2.5}$ with the USII (Figures 11b and 11c), $PM_{2.5}$ concentration significantly reduces the USII and inhibited the heat exchange between urban and rural areas in winter, indirectly changes the $UHII$. The results of the analysis of the sounding data show that, the accumulation of pollutants influences the vertical temperature gradient and weakens the vertical convective motion (Figures 12a and 12b), resulting in the great reduction of TLR and even the appearance of temperature inversion layer in winter (Figure 12c). The stable boundary layer becomes lower (Figure 12d) and the lower-layer atmosphere tends to stabilize (Figure 12e), which reduces the horizontal and vertical convection of air and weakens the horizontal wind speed. Horizontal convection and wind affect the heat exchange between urban and rural areas and make heat accumulate in the urban area. The weakening of vertical convection hinders the upward movement of the urban atmosphere, and the difficulty of heat diffusion through the upper layer leads to further accumulation, which enhances the urban heat island. Figure 13b conceptualizes the influence of aerosols on

UHII in winter. However, seasonal differences also exist. The above process is not obvious in summer, and this effect is much stronger in winter. The boundary layer effect caused by aerosol is not the main factor affecting the UHII variation in summer.

4.3. Evaporative Pathway and Climate Background

Evaporation is another factor that affects temperature in the process of urbanization. With the development of cities, impervious surfaces have replaced vegetation and soil, which reduce evaporation sources. Observations confirm that daytime evaporation is smaller in most cities than in their surrounding countryside (Oke et al., 2017). Evaporation is also directly related to radiation and wind (Liu, 2004), and is indirectly affected by aerosols (Roderick & Farquhar, 2002). In Figure 9, PM_{2.5} makes the pan-evaporation decline faster in urban than in rural areas, which decreases the latent heat flux and increases sensible heat flux in urban areas, resulting in a stronger UHII. In summer, due to the stronger solar radiation, the influence of aerosols on the surface and air temperature through radiation is higher than through evaporation, so the overall effect is the reduction of UHII. In winter, temperature change caused by evaporation may also be one of the reasons for the enhancement of UHII during daytime, which acts together with radiation effect. In addition, aerosols reduce evaporation difference between urban and rural areas in winter more than in summer. This means that, compared with urban areas in the same season, attenuation effect of aerosols on rural evaporation is weaker in winter than in summer. It is also possible that the enhancement of evaporation via diffuse radiation-enhanced-photosynthesis plays an important role here. More diffuse radiation strengthens the photosynthesis of vegetation, and more evaporation is produced through transpiration, which offsets the evaporation loss caused by the reduction of direct radiation. The energy consumed by transpiration further reduces the surface and air temperature in rural areas and promotes the development of UHI.

Furthermore, there are other factors that alter the effect of aerosol on UHII by simultaneously influencing aerosol and the UHI, such as the geographic and climate background of the city. As shown in Figure 10, due to the geographical feature of Beijing's gradual reduction of pollutants from south to north, the effects of different seasonal wind directions are important and completely opposite. Southeast (southwest) wind in summer increases pollution and reduces the UHI, resulting in a negative correlation of pollutants and UHII. Northwest wind in winter simultaneously reduces or enhances air pollution and UHII, causing a positive correlation of them. The impact of wind on pollutants and UHII needs to be further considered.

5. Conclusions

Based on the ground and sounding data from 2016 to 2018, this paper examines the relationships between PM_{2.5} concentration and the UHI intensity in Beijing. PM_{2.5} weakens the UHII in summer but strengthens it in winter. Meantime PM_{2.5} lessens the UHII at night. These effects can be explained by aerosol radiation interaction (direct effect) and aerosol-PBL interaction (indirect effect).

During the summer daytime, particles have little influence on PBL, the main effect of PM_{2.5} on UHII is aerosol radiation interaction and aerosol evaporation effect, the former has a greater impact. The urban-rural radiation difference caused by the uneven spatial distribution of PM_{2.5} is the important reason for the reduction of urban heat island.

During the winter daytime, pollution in both urban and rural areas is serious. In one aspect, more emission and distribution of absorbent aerosols makes urban areas more capable of heating the atmosphere, enhances UHII. On the other hand, under the influence of particles and the PBL, the atmosphere tends to be more stabilized in pollution condition, convection weakened. Heat accumulates in urban areas and enhances UHII. Moreover, increased evaporation in rural areas caused by diffuse radiation-enhanced-photosynthesis of PM_{2.5} increases the temperature difference between urban and rural areas. PM_{2.5} affects urban heat island through evaporation pathway, radiation interaction and the PBL interaction, with the latter having a higher impact.

At night, aerosol radiation interaction indirectly affects the change of UHII. High-concentration aerosols reduce the solar radiant energy received, stored during daytime and released at night by the ground and urban canopy, make urban areas relatively more "cool" than rural areas and weakens the urban heat island.

Our current work improves the understanding of urban climate affected by air pollution and may provide a scientific basis for mitigating the impact of UHI on Beijing. However, due to Beijing's unique geographical location, terrain and climate background, industrial distribution and other factors, our research results cannot be fully applicable to all cities. However, we believe that these findings should also have important implications for other urban areas suffering from severe air pollution. Furthermore, among the possible mechanisms mentioned, many of them act in the same direction. It is somehow difficult to separate the mechanisms merely applying statistical procedure, and numerical simulation should be taken to further examine the contributions of the influential factors.

Data Availability Statement

The land use data of mainland China are provided by the Resources and Environmental Sciences Data Center, Chinese Academy of Sciences (www.resdc.cn/data.aspx?DATAID=184). The daily surface air temperature data set of automatic weather station and hourly radiation, L-band sounding data are provided by the National Meteorological Information Center (NMIC), China Meteorological Administration (CMA) (http://10.20.76.55/cimissapiweb/apidataclassdefine_list.action), the data itself are confidential and cannot be provided or made public in accordance with national laws, the corresponding author can be contacted if necessary. The PM_{2.5} data are available on the website of Beijing Municipal Ecological and Environmental Monitoring center (<http://www.bjmcmc.com.cn/>) and Ministry of Ecology and Environmental of the People's Republic of China (<http://106.37.208.233:20035>).

Acknowledgments

This study is supported by the National Key Research and Development Program of China (2018YFA0605603).

References

- Alonso, M., Fidalgo, M., & Labajo, J. (2007). The urban heat island in Salamanca (Spain) and its relationship to meteorological parameters. *Climate Research*, 34, 39–46. <https://doi.org/10.3354/cr034039>
- Bright, R. M., Davin, E., O'Halloran, T., Pongratz, J., Zhao, K., & Cescatti, A. (2017). Local temperature response to land cover and management change driven by non-radiative processes. *Nature Climate Change*, 7(4), 296–302. <https://doi.org/10.1038/nclimate3250>
- Cao, C., Lee, X., Liu, S., Schultz, N., Xiao, W., Zhang, M., & Zhao, L. (2016). Urban heat islands in China enhanced by haze pollution. *Nature Communications*, 7(1), 12509. <https://doi.org/10.1038/ncomms12509>
- Chakraborty, T., & Lee, X. (2019). Land cover regulates the spatial variability of temperature response to the direct radiative effect of aerosols. *Geophysical Research Letters*, 46(15), 8995–9003. <https://doi.org/10.1029/2019GL083812>
- Chakraborty, T., Lee, X., & Lawrence, D. M. (2021). Strong local evaporative cooling over land due to atmospheric aerosols. *Journal of Advances in Modeling Earth Systems*, 13(5), e2021MS002491. <https://doi.org/10.1029/2021MS002491>
- Chakraborty, T., Sarangi, C., & Lee, X. (2021). Reduction in human activity can enhance the urban heat island: Insights from the COVID-19 lockdown. *Environmental Research Letters*, 16(5), 054060. <https://doi.org/10.1088/1748-9326/abef8e>
- Chakraborty, T., Sarangi, C., & Tripathi, S. N. (2017). Understanding diurnality and inter-seasonality of a sub-tropical urban heat island. *Boundary-Layer Meteorology*, 163(2), 287–309. <https://doi.org/10.1007/s10546-016-0223-0>
- Chen, L., Zhang, M., Zhu, J., Wang, Y., & Skorokhod, A. (2018). Modeling impacts of urbanization and urban heat island mitigation on boundary layer meteorology and air quality in Beijing under different weather conditions. *Journal of Geophysical Research: Atmospheres*, 123(8), 4323–4344. <https://doi.org/10.1002/2017JD027501>
- Chen, L., Zhu, W., Zhou, X., & Zhou, Z. (2003). Characteristics of the heat island effect in Shanghai and its possible mechanism. *Advances in Atmospheric Sciences*, 20(6), 991–1001. <https://doi.org/10.1007/BF02915522>
- Clinton, N., & Gong, P. (2013). MODIS detected surface urban heat islands and sinks: Global locations and controls. *Remote Sensing of Environment*, 134, 294–304. <https://doi.org/10.1016/j.rse.2013.03.008>
- Cohen, A. J., Brauer, M., Burnett, R., Anderson, H. R., Frostad, J., Estep, K., et al. (2017). Estimates and 25-year trends of the global burden of disease attributable to ambient air pollution: An analysis of data from the global burden of diseases study 2015. *The Lancet*, 389(10082), 1907–1918. [https://doi.org/10.1016/S0140-6736\(17\)30505-6](https://doi.org/10.1016/S0140-6736(17)30505-6)
- Crutzen, P. (2004). New directions: The growing urban heat and pollution island effect impact—On chemistry and climate. *Atmospheric Environment*, 38(21), 3539–3540. <https://doi.org/10.1016/j.atmosenv.2004.03.032>
- Ding, A. J., Huang, X., Nie, W., Sun, J. N., Kerminen, V.-M., Petäjä, T., et al. (2016). Enhanced haze pollution by black carbon in megacities in China. *Geophysical Research Letters*, 43(6), 2873–2879. <https://doi.org/10.1002/2016GL067745>
- Durant, J. L., Lafleur, A. L., Busby, W. F., Donhoffner, L. L., Penman, B. W., & Crespi, C. L. (1999). Mutagenicity of C₂₄H₁₄ PAH in human cells expressing CYP1A1. *Mutation Research: Genetic Toxicology and Environmental Mutagenesis*, 446(1), 1–14. [https://doi.org/10.1016/S1383-5718\(99\)00135-7](https://doi.org/10.1016/S1383-5718(99)00135-7)
- Gabriel, K. M. A., & Endlicher, W. R. (2011). Urban and rural mortality rates during heat waves in Berlin and Brandenburg, Germany. *Environmental Pollution*, 159(8–9), 2044–2050. <https://doi.org/10.1016/j.envpol.2011.01.016>
- Gu, L., Baldocchi, D., Verma, S. B., Black, T. A., Vesala, T., Falge, E. M., & Dowty, P. R. (2002). Advantages of diffuse radiation for terrestrial ecosystem productivity. *Journal of Geophysical Research*, 107(D6). <https://doi.org/10.1029/2001JD001242>
- Gu, Y., Liou, K. N., Chen, W., & Liao, H. (2010). Direct climate effect of black carbon in China and its impact on dust storms. *Journal of Geophysical Research*, 115, D00K14. <https://doi.org/10.1029/2009JD013427>
- Hamilton, R. S., & Mansfield, T. A. (1991). Airborne particulate elemental carbon: Its sources, transport and contribution to dark smoke and soiling. *Atmospheric Environment Part A. General Topics*, 25(3–4), 715–723. [https://doi.org/10.1016/0960-1686\(91\)90070-N](https://doi.org/10.1016/0960-1686(91)90070-N)
- Han, W., Li, Z., Wu, F., Zhang, Y., Guo, J., Su, T., et al. (2020). The mechanisms and seasonal differences of the impact of aerosols on daytime surface urban heat island effect. *Atmospheric Chemistry and Physics*, 20(11), 6479–6493. <https://doi.org/10.5194/acp-20-6479-2020>

- He, Y., & Wang, K. (2020). Contrast patterns and trends of lapse rates calculated from near-surface air and land surface temperatures in China from 1961 to 2014. *Science Bulletin*, 65(14), 1217–1224. <https://doi.org/10.1016/j.scib.2020.04.001>
- Holden, J., & Rose, R. (2011). Temperature and surface lapse rate change: A study of the UK's longest upland instrumental record. *International Journal of Climatology*, 31(6), 907–919. <https://doi.org/10.1002/joc.2136>
- Hou, A., Ni, G., Yang, H., & Lei, Z. (2013). Numerical analysis on the contribution of urbanization to wind stilling: An example over the greater Beijing metropolitan area. *Journal of Applied Meteorology and Climatology*, 52(5), 1105–1115. <https://doi.org/10.1175/JAMC-D-12-013.1>
- Huang, J., Wang, T., Wang, W., Li, Z., & Yan, H. (2014). Climate effects of dust aerosols over East Asian arid and semiarid regions. *Journal of Geophysical Research: Atmospheres*, 119(19), 11398–11416. <https://doi.org/10.1002/2014JD021796>
- Huang, X., Wang, Z., & Ding, A. (2018). Impact of Aerosol-PBL interaction on haze pollution: Multiyear observational evidences in North China. *Geophysical Research Letters*, 45(16), 8596–8603. <https://doi.org/10.1029/2018GL079239>
- Huebert, B. J. (2003). An overview of ACE-Asia: Strategies for quantifying the relationships between Asian aerosols and their climatic impacts. *Journal of Geophysical Research*, 108(D23), 8633. <https://doi.org/10.1029/2003JD003550>
- Imhoff, M. L., Zhang, P., Wolfe, R. E., & Bouyoucos, L. (2010). Remote sensing of the urban heat island effect across biomes in the continental USA. *Remote Sensing of Environment*, 114(3), 504–513. <https://doi.org/10.1016/j.rse.2009.10.008>
- Jacobson, M. Z. (1998). Studying the effects of aerosols on vertical photolysis rate coefficient and temperature profiles over an urban airshed. *Journal of Geophysical Research*, 103(D9), 10593–10604. <https://doi.org/10.1029/98JD00287>
- Jia, W., Ren, G., Kan-zhuo, S., Zhang, P., Wen, K., & Ren, Y. (2019). Urban heat island effect and its contribution to observed temperature increase at Wuhan station, Central China. *Journal of Tropical Meteorology*, 12.
- Jin, M., & Dickinson, R. E. (2010). Land surface skin temperature climatology: Benefiting from the strengths of satellite observations. *Environmental Research Letters*, 5(4), 044004. <https://doi.org/10.1088/1748-9326/5/4/044004>
- Jin, M., Dickinson, R. E., & Vogelmann, A. M. (1997). A comparison of CCM2-BATS skin temperature and surface-air temperature with satellite and surface observations. *Journal of Climate*, 10, 20. [https://doi.org/10.1175/1520-0442\(1997\)010<0020:ACOCBS>2.0.CO;2](https://doi.org/10.1175/1520-0442(1997)010<0020:ACOCBS>2.0.CO;2)
- Jin, M., Kessomkiat, W., & Pereira, G. (2011). Satellite-observed urbanization characters in Shanghai, China: Aerosols, urban heat island effect, and land-atmosphere interactions. *Remote Sensing*, 3(1), 83–99. <https://doi.org/10.3390/rs3010083>
- Jin, M., & Shepherd, J. M. (2005). Inclusion of Urban landscape in a climate model: How can satellite data help? *Bulletin of the American Meteorological Society*, 86(5), 681–690. <https://doi.org/10.1175/BAMS-86-5-681>
- Jin, M., Shepherd, J. M., & Zheng, W. (2010). Urban surface temperature reduction via the Urban aerosol direct effect: A remote sensing and WRF model sensitivity study. *Advances in Meteorology*, 2010, 1–14. <https://doi.org/10.1155/2010/681587>
- Jones, G. S., Christidis, N., & Stott, P. A. (2011). Detecting the influence of fossil fuel and bio-fuel black carbon aerosols on near surface temperature changes. *Atmospheric Chemistry and Physics*, 11(2), 799–816. <https://doi.org/10.5194/acp-11-799-2011>
- Jonsson, P., Bennet, C., Eliasson, I., & Selin Lindgren, E. (2004). Suspended particulate matter and its relations to the urban climate in Dar es Salaam, Tanzania. *Atmospheric Environment*, 38(25), 4175–4181. <https://doi.org/10.1016/j.atmosenv.2004.04.021>
- Kalnay, E., & Cai, M. (2003). Impact of urbanization and land-use change on climate. *Nature*, 423(6939), 528–531. <https://doi.org/10.1038/nature01675>
- Kuhlbusch, T. A. J. (1998). Black carbon and the carbon cycle. *Science*, 280(5371), 1903–1904. <https://doi.org/10.1126/science.280.5371.1903>
- Künzli, N., Kaiser, R., Medina, S., Studnicka, M., Chanel, O., Filliger, P., et al. (2000). Public-health impact of outdoor and traffic-related air pollution: A European assessment. *The Lancet*, 356(9232), 795–801. [https://doi.org/10.1016/S0140-6736\(00\)02653-2](https://doi.org/10.1016/S0140-6736(00)02653-2)
- Lai, L.-W., & Cheng, W.-L. (2010). Urban heat island and air pollution—an emerging role for hospital respiratory admissions in an urban area. *Journal of Environmental Health*, 72(6), 32–35.
- Li, H., Meier, F., Lee, X., Chakraborty, T., Liu, J., Schaap, M., & Sodoudi, S. (2018). Interaction between urban heat island and urban pollution island during summer in Berlin. *The Science of the Total Environment*, 636, 818–828. <https://doi.org/10.1016/j.scitotenv.2018.04.254>
- Li, H., Sodoudi, S., Liu, J., & Tao, W. (2020). Temporal variation of urban aerosol pollution island and its relationship with urban heat island. *Atmospheric Research*, 241, 104957. <https://doi.org/10.1016/j.atmosres.2020.104957>
- Li, L., Wang, Y., Zhang, Q., Yu, T., Zhao, Y., & Jin, J. (2007). Spatial distribution of aerosol pollution based on MODIS data over Beijing, China. *Journal of Environmental Sciences*, 19(8), 955–960. [https://doi.org/10.1016/S1001-0742\(07\)60157-0](https://doi.org/10.1016/S1001-0742(07)60157-0)
- Li, Z., Guo, J., Ding, A., Liao, H., Liu, J., Sun, Y., et al. (2017). Aerosol and boundary-layer interactions and impact on air quality. *National Science Review*, 4(6), 810–833. <https://doi.org/10.1093/nsr/nwx117>
- Li, Z., Niu, F., Fan, J., Liu, Y., Rosenfeld, D., & Ding, Y. (2011). Long-term impacts of aerosols on the vertical development of clouds and precipitation. *Nature Geoscience*, 4(12), 888–894. <https://doi.org/10.1038/ngeo1313>
- Liu, B. (2004). A spatial analysis of pan evaporation trends in China, 1955–2000. *Journal of Geophysical Research*, 109(D15), D15102. <https://doi.org/10.1029/2004JD004511>
- Liu, S., & Liang, X.-Z. (2010). Observed diurnal cycle climatology of planetary boundary layer height. *Journal of Climate*, 23(21), 5790–5809. <https://doi.org/10.1175/2010JCLI3552.1>
- McDonnell, M. J., & MacGregor-Fors, I. (2016). The ecological future of cities. *Science*, 352(6288), 936–938. <https://doi.org/10.1126/science.aaf3630>
- Menon, S. (2002). Climate effects of black carbon aerosols in China and India. *Science*, 297(5590), 2250–2253. <https://doi.org/10.1126/science.1075159>
- Mildrexler, D. J., Zhao, M., & Running, S. W. (2011). A global comparison between station air temperatures and MODIS land surface temperatures reveals the cooling role of forests. *Journal of Geophysical Research*, 116(G3), G03025. <https://doi.org/10.1029/2010JG001486>
- Monteith, J. L., & Oke, T. R. (1980). Boundary layer climates. *The Journal of Applied Ecology*, 17(2), 517. <https://doi.org/10.2307/2402350>
- Murthy, B. S., Latha, R., Kumar, M., & Mahanti, N. C. (2014). Effect of aerosols on evapo-transpiration. *Atmospheric Environment*, 89, 109–118. <https://doi.org/10.1016/j.atmosenv.2014.02.029>
- Oke, T. R. (1976). The distinction between canopy and boundary-layer urban heat islands. *Atmosphere*, 14(4), 268–277. <https://doi.org/10.1080/00046973.1976.9648422>
- Oke, T. R. (1982). The energetic basis of the urban heat island. *Quarterly Journal of the Royal Meteorological Society*, 108(455), 1–24. <https://doi.org/10.1002/qj.49710845502>
- Oke, T. R., Mills, G., Christen, A., & Voogt, J. A. (2017). *Urban climates*. Cambridge: Cambridge University Press. <https://doi.org/10.1017/978139016476>
- Pandey, P., Kumar, D., Prakash, A., Masih, J., Singh, M., Kumar, S., et al. (2012). A study of urban heat island and its association with particulate matter during winter months over Delhi. *The Science of the Total Environment*, 414, 494–507. <https://doi.org/10.1016/j.scitotenv.2011.10.043>

- Peng, J., Ma, J., Liu, Q., Liu, Y., Hu, Y., Li, Y., & Yue, Y. (2018). Spatial-temporal change of land surface temperature across 285 cities in China: An urban-rural contrast perspective. *The Science of the Total Environment*, 635, 487–497. <https://doi.org/10.1016/j.scitotenv.2018.04.105>
- Peng, S., Piao, S., Ciais, P., Friedlingstein, P., Ottle, C., Bréon, F.-M., et al. (2012). Surface urban heat island across 419 global big cities. *Environmental Science & Technology*, 46(2), 696–703. <https://doi.org/10.1021/es2030438>
- Poupkou, A., Nastos, P., Melas, D., & Zerefos, C. (2011). Climatology of discomfort index and air quality index in a large urban mediterranean agglomeration. *Water, Air, & Soil Pollution*, 222(1–4), 163–183. <https://doi.org/10.1007/s11270-011-0814-9>
- Qin, Y., Ren, G., Huang, Y., Zhang, P., & Wen, K. (2021). Application of geographically weighted regression model in the estimation of surface air temperature lapse rate. *Journal of Geographical Sciences*, 31(3), 389–402. <https://doi.org/10.1007/s11442-021-1849-5>
- Ramanathan, V., Crutzen, P. J., Lelieveld, J., Mitra, A. P., Althausen, D., Anderson, J., et al. (2001). Indian Ocean experiment: An integrated analysis of the climate forcing and effects of the great Indo-Asian haze. *Journal of Geophysical Research*, 106(D22), 28371–28398. <https://doi.org/10.1029/2001JD900133>
- Rasch, P. J., Collins, W. D., & Eaton, B. E. (2001). Understanding the Indian Ocean experiment (INDOEX) aerosol distributions with an aerosol assimilation. *Journal of Geophysical Research*, 106(D7), 7337–7355. <https://doi.org/10.1029/2000JD900508>
- Ren, G., & Zhou, Y. (2014). Urbanization effect on trends of extreme temperature indices of national stations over Mainland China, 1961–2008. *Journal of Climate*, 27(6), 2340–2360. <https://doi.org/10.1175/JCLI-D-13-00393.1>
- Ren, G., Zhou, Y., Chu, Z., Zhou, J., Zhang, A., Guo, J., & Liu, X. (2008). Urbanization effects on observed surface air temperature trends in North China. *Journal of Climate*, 21(6), 1333–1348. <https://doi.org/10.1175/2007JCLI1348.1>
- Ren, Z., & Xiong, A. (2007). Operational system development on three-step quality control of observations from AWS (in Chinese). *Meteorological Monthly*, 33(01), 19–24.
- Ren, Z., Zhang, Z., Sun, C., Liu, Y., Li, J., Ju, X., et al. (2015). Development of three-step quality control system of real-time observation data from AWS in China (in Chinese). *Meteorological Monthly*, 41(10), 1268–1277. <https://doi.org/10.7519/j.issn.1000-0526.2015.10.010>
- Rizwan, A. M., Dennis, L. Y. C., & Liu, C. (2008). A review on the generation, determination and mitigation of urban heat island. *Journal of Environmental Sciences*, 20(1), 120–128. [https://doi.org/10.1016/S1001-0742\(08\)60019-4](https://doi.org/10.1016/S1001-0742(08)60019-4)
- Roderick, M. L., & Farquhar, G. D. (2002). The cause of decreased pan evaporation over the past 50 years. *Science*, 298(5597), 1410–1411. <https://doi.org/10.1126/science.1075390-a>
- Rosen, H., Hansen, A. D. A., Gundel, L., & Novakov, T. (1978). Identification of the optically absorbing component in urban aerosols. *Applied Optics*, 17(24), 3859–3861. <https://doi.org/10.1364/AO.17.003859>
- Rosenfeld, D., Lohmann, U., Raga, G. B., O'Dowd, C. D., Kulmala, M., Fuzzi, S., et al. (2008). Flood or drought: How do aerosols affect precipitation? *Science*, 321(5894), 1309–1313. <https://doi.org/10.1126/science.1160606>
- Rosenzweig, C., Solecki, W. D., Parshall, L., Chopping, M., Pope, G., & Goldberg, R. (2005). Characterizing the urban heat island in current and future climates in New Jersey. *Environmental Hazards*, 6(1), 51–62. <https://doi.org/10.1016/j.hazards.2004.12.001>
- Ryu, Y.-H., & Baik, J.-J. (2012). Quantitative analysis of factors contributing to urban heat island intensity. *Journal of Applied Meteorology and Climatology*, 51(5), 842–854. <https://doi.org/10.1175/JAMC-D-11-098.1>
- Sang, J., Liu, H., Liu, H., & Zhang, Z. (2000). Observational and numerical studies of wintertime urban boundary layer. *Journal of Wind Engineering and Industrial Aerodynamics*, 87(2–3), 243–258. [https://doi.org/10.1016/S0167-6105\(00\)00040-4](https://doi.org/10.1016/S0167-6105(00)00040-4)
- Sarrat, C., Lemonsu, A., Masson, V., & Guedalia, D. (2006). Impact of urban heat island on regional atmospheric pollution. *Atmospheric Environment*, 40(10), 1743–1758. <https://doi.org/10.1016/j.atmosenv.2005.11.037>
- Shepherd, J. M., Carter, M., Manyin, M., Messen, D., & Burian, S. (2010). The impact of urbanization on current and future coastal precipitation: A case study for Houston. *Environment and Planning B: Planning and Design*, 37(2), 284–304. <https://doi.org/10.1068/b34102t>
- Taha, H. (1997). Urban climates and heat islands: Albedo, evapotranspiration, and anthropogenic heat. *Energy and Buildings*, 25(2), 99–103. [https://doi.org/10.1016/S0378-7788\(96\)00999-1](https://doi.org/10.1016/S0378-7788(96)00999-1)
- Travis, D. J., Carleton, A. M., & Lauritsen, R. G. (2002). Contrails reduce daily temperature range. *Nature*, 418(6898), 601–601. <https://doi.org/10.1038/418601a>
- Voogt, J. A., & Oke, T. R. (2003). Thermal remote sensing of urban climates. *Remote Sensing of Environment*, 86(3), 370–384. [https://doi.org/10.1016/S0034-4257\(03\)00079-8](https://doi.org/10.1016/S0034-4257(03)00079-8)
- Wang, J., Qiu, Y., He, S., Liu, N., Xiao, C., & Liu, L. (2018). Investigating the driving forces of NO_x generation from energy consumption in China. *Journal of Cleaner Production*, 184, 836–846. <https://doi.org/10.1016/j.jclepro.2018.02.305>
- Wang, K., Dickinson, R. E., & Liang, S. (2008). Observational evidence on the effects of clouds and aerosols on net ecosystem exchange and evapotranspiration. *Geophysical Research Letters*, 35(10), L10401. <https://doi.org/10.1029/2008GL034167>
- Wang, K., Jiang, S., Wang, J., Zhou, C., Wang, X., & Lee, X. (2017). Comparing the diurnal and seasonal variabilities of atmospheric and surface urban heat islands based on the Beijing urban meteorological network. *Journal of Geophysical Research: Atmospheres*, 122(4), 2131–2154. <https://doi.org/10.1002/2016JD025304>
- Wu, H., Wang, T., Riemer, N., Chen, P., Li, M., & Li, S. (2017). Urban heat island impacted by fine particles in Nanjing, China. *Scientific Reports*, 7(1), 11422. <https://doi.org/10.1038/s41598-017-11705-z>
- Wu, H., Wang, T., Wang, Q., Cao, Y., Qu, Y., & Nie, D. (2021). Radiative effects and chemical compositions of fine particles modulating urban heat island in Nanjing, China. *Atmospheric Environment*, 247, 118201. <https://doi.org/10.1016/j.atmosenv.2021.118201>
- Yang, P., Ren, G., & Liu, W. (2013). Spatial and temporal characteristics of Beijing urban heat island intensity. *Journal of Applied Meteorology and Climatology*, 52(8), 1803–1816. <https://doi.org/10.1175/JAMC-D-12-0125.1>
- Yang, P., Ren, G., & Yan, P. (2017). Evidence for a strong association of short-duration intense rainfall with urbanization in the Beijing urban area. *Journal of Climate*, 30(15), 5851–5870. <https://doi.org/10.1175/JCLI-D-16-0671.1>
- Yang, P., Ren, G., Yan, P., & Deng, J. (2020). Tempospatial pattern of surface wind speed and the “Urban Stilling Island” in Beijing city. *Journal of Meteorological Research*, 34(5), 986–996. <https://doi.org/10.1007/s13351-020-9135-5>
- Yang, Q., Huang, X., & Tang, Q. (2019). The footprint of urban heat island effect in 302 Chinese cities: Temporal trends and associated factors. *The Science of the Total Environment*, 655, 652–662. <https://doi.org/10.1016/j.scitotenv.2018.11.171>
- Yang, X., Li, Y., Luo, Z., & Chan, P. W. (2017). The urban cool island phenomenon in a high-rise high-density city and its mechanisms. *International Journal of Climatology*, 37(2), 890–904. <https://doi.org/10.1002/joc.4747>
- Yang, Y., Zheng, Z., Yim, S. Y. L., Roth, M., Ren, G., Gao, Z., et al. (2020). PM_{2.5} pollution modulates wintertime urban heat island intensity in the Beijing-Tianjin-Hebei megalopolis, China. *Geophysical Research Letters*, 47(1), e2019GL084288. <https://doi.org/10.1029/2019GL084288>
- Yao, R., Wang, L., Huang, X., Niu, Z., Liu, F., & Wang, Q. (2017). Temporal trends of surface urban heat islands and associated determinants in major Chinese cities. *The Science of the Total Environment*, 609, 742–754. <https://doi.org/10.1016/j.scitotenv.2017.07.217>

- Yao, R., Wang, L., Huang, X., Zhang, W., Li, J., & Niu, Z. (2018). Interannual variations in surface urban heat island intensity and associated drivers in China. *Journal of Environmental Management*, 222, 86–94. <https://doi.org/10.1016/j.jenvman.2018.05.024>
- Yu, M., Tang, G., Yang, Y., Li, Q., Wang, Y., Miao, S., et al. (2020). The interaction between urbanization and aerosols during a typical winter haze event in Beijing. *Atmospheric Chemistry and Physics*, 20(16), 9855–9870. <https://doi.org/10.5194/acp-20-9855-2020>
- Zhang, H., Zhang, B., Lv, M., & An, L. (2017). Development and application of stable weather index of Beijing in environmental meteorology (in Chinese). *Meteorological Monthly*, 43(08), 998–1004. <https://doi.org/10.7519/j.issn.1000-0526.2017.08.010>
- Zhang, Y., Li, F., & Liu, M. (2004). Analysis on urban heat island changing trend and its relation with TSP in Shenyang (in Chinese). *Environmental Protection Science*, 02, 1–2+8. <https://doi.org/10.16803/j.cnki.issn.1004-6216.2004.02.001>
- Zhao, L., Lee, X., Smith, R. B., & Oleson, K. (2014). Strong contributions of local background climate to urban heat islands. *Nature*, 511(7508), 216–219. <https://doi.org/10.1038/nature13462>
- Zheng, Z., Ren, G., Wang, H., Dou, J., Gao, Z., Duan, C., et al. (2018). Relationship between fine-particle pollution and the urban heat island in Beijing, China: Observational evidence. *Boundary-Layer Meteorology*, 169(1), 93–113. <https://doi.org/10.1007/s10546-018-0362-6>
- Zhou, D., Zhang, L., Hao, L., Sun, G., Liu, Y., & Zhu, C. (2016). Spatiotemporal trends of urban heat island effect along the urban development intensity gradient in China. *The Science of the Total Environment*, 544, 617–626. <https://doi.org/10.1016/j.scitotenv.2015.11.168>
- Zhou, D., Zhao, S., Liu, S., Zhang, L., & Zhu, C. (2014). Surface urban heat island in China's 32 major cities: Spatial patterns and drivers. *Remote Sensing of Environment*, 152, 51–61. <https://doi.org/10.1016/j.rse.2014.05.017>
- Zhou, S., & Zheng, J. (1991). The turbidity island effect in Shanghai urban climate. *Energy and Buildings*, 16(1–2), 657–662. [https://doi.org/10.1016/0378-7788\(91\)90034-Z](https://doi.org/10.1016/0378-7788(91)90034-Z)